

8-2008

# Accelerated Life Testing of Electronic Revenue Meters

Venkata Chaluvadi

Clemson University, cvnharish@gmail.com

Follow this and additional works at: [https://tigerprints.clemson.edu/all\\_theses](https://tigerprints.clemson.edu/all_theses)



Part of the [Electrical and Computer Engineering Commons](#)

---

## Recommended Citation

Chaluvadi, Venkata, "Accelerated Life Testing of Electronic Revenue Meters" (2008). *All Theses*. 470.

[https://tigerprints.clemson.edu/all\\_theses/470](https://tigerprints.clemson.edu/all_theses/470)

This Thesis is brought to you for free and open access by the Theses at TigerPrints. It has been accepted for inclusion in All Theses by an authorized administrator of TigerPrints. For more information, please contact [kokeefe@clemson.edu](mailto:kokeefe@clemson.edu).

ACCELERATED LIFE TESTING OF ELECTRONIC REVENUE METERS

---

A Thesis  
Presented to  
the Graduate School of  
Clemson University

---

In Partial Fulfillment  
of the Requirements for the Degree  
Master of Science  
Electrical Engineering

---

by  
Venkata Naga Harish Chaluvadi  
December 2008

---

Accepted by:  
Dr. E. Randolph Collins, Committee Chair  
Dr. Elham B. Makram  
Dr. Michael Bridgwood

## ABSTRACT

Electricity meters are devices that continuously record electrical energy consumption. In the past, meters have been of electromechanical type and consisted windings and moving parts. Electromechanical meters tend to be bulky, less accurate and more susceptible to tampering. As with other aging power system infrastructure in the US, most electricity meters are around 40 years old and are nearing the end of their intended lifespan. Concerns over the accuracy of these electromechanical meters along with advances in technology have led to development of new electronic meters which have additional benefits such as light weight, tamper-proof mechanisms, harmonic detection and Advanced Metering Infrastructure (AMI) features. Utilities intend to spend millions of dollars over the next few years in replacing these aging electromechanical meters; however the new meters contain electronic parts that are typically more sensitive to environmental conditions and abnormal voltage conditions. The drive to replace older meters will not meet the expectations, either in terms of functionality or expected profits, if the new meters drift in accuracy or fail relatively quickly with respect to their electromechanical counterparts.

This thesis discusses the methods and techniques used in industry to perform reliability and accelerated life testing analysis and such a study is performed on electronic meters to predict their life. Industry standards are reviewed and accelerated test plans are developed to systematically study the effect of environmental stresses on electronic revenue meters by using failure time distributions, degradation parameters and

accelerating factors to predict their life. A Human Machine Interface (HMI) was developed in LabVIEW to interface the data acquisition devices with software, and thus facilitate continuous monitoring of environmental parameters and the health of test specimens placed inside an environmental chamber. The HMI also has the capability of generating automated periodic reports and emails for review by management.

Since the lab test data from accelerated life testing of electronic meters was yet to be obtained, the statistical analysis procedure, derived from the literature review, was demonstrated using ALT data from other electrical and electronic components. ALT data for cable insulation was obtained from the literature, and the failure data analysis to predict the relation between cable life and temperature was demonstrated. Another example illustrating degradation analysis using degradation data of LEDs, using current as an accelerating stress, was provided. Finally, the causes for lack of data were analyzed and improvements in testing procedure were recommended.

## ACKNOWLEDGMENTS

I would like to sincerely thank Dr. E. Randolph Collins for his guidance, motivation and patience throughout my Masters program. Without his support, none of this would have been possible. I would like to thank Dr. Elham B. Makram and Dr. Michael Bridgwood for their support as instructors and for serving on my committee.

I thank Mr. Charles Perry of Electric Power Research Institute (EPRI) for providing this project topic and research grant for the support of my thesis and the PQIA lab.

I would also like to thank Curtiss Fox and Daniel Fain for their advice and assistance in the lab.

Finally I would like to thank my parents whose continuous love and encouragement have got me through stressful times.

## TABLE OF CONTENTS

	Page
TITLE PAGE .....	i
ABSTRACT.....	ii
ACKNOWLEDGMENTS .....	iv
LIST OF TABLES .....	vii
LIST OF FIGURES .....	viii
CHAPTER	
1. INTRODUCTION .....	1
2. OVERVIEW OF METERING TECHNOLOGY .....	6
Introduction.....	6
Electromechanical meters .....	6
Electronic meters .....	11
Advanced Metering Infrastructure .....	15
Meter testing and calibration .....	17
3. RELIABILITY AND ACCELERATED LIFE TESTING .....	20
Introduction.....	20
Data types.....	23
Statistical analysis .....	25
Test plans .....	42
4. DATA ACQUISITION SYSTEM.....	43
Introduction .....	43
Data Acquisition system .....	46
Energy and power measurement.....	47
Temperature measurement.....	59
Prototype .....	64
Original system at EPRI.....	67
Human Machine Interface.....	71

Table of contents (continued)

5.	TEST PLAN, RESULTS AND DISCUSSION .....	83
	Test procedure.....	83
	Test results and discussion.....	85
	Recommended test plan .....	87
6.	ANALYSIS USING EXAMPLES .....	89
	Introduction.....	89
	Failure data analysis.....	90
	Degradation analysis.....	100
7.	CONCLUSION.....	104
	Future work.....	107
	APPENDICES .....	109
	A: NI SCB 68 breakout board pin diagram .....	110
	B: Type T thermocouple coefficients .....	111
	C: LabVIEW program .....	112
	REFERENCES .....	117

## LIST OF TABLES

Table	Page
3.1 Failure mechanisms and related stresses.....	23
4.1 Acquisition devices used for the project.....	47
4.2 List of thermocouple types with characteristics.....	61
6.1 Failure data of insulation specimens.....	91
6.2 Anderson Darling test statistic values.....	97
6.3 Degradation data of LEDs .....	101



## LIST OF FIGURES

Figure		Page
2.1	Front view of an electromechanical watt-hour meter .....	7
2.2	Components of a single-phase induction watt-hour meter .....	8
2.3	Vector diagram of the operating quantities in a watt-hour meter .....	9
2.4	Front view of an electronic watt-hour meter.....	12
2.5	Schematic of an electronic watt-hour meter .....	14
2.6	Internal components of an electronic watt-hour meter .....	14
2.7	Schematic of an electronic watt-hour meter with AMR .....	16
2.8	UTEK 5600 Universal Calibration device .....	18
2.9	Sample Utility meter calibration report .....	19
3.1	Effect of $\lambda$ on the pdf of an exponential distribution.....	26
3.2	Effect of $\lambda$ on the cdf of an exponential distribution.....	27
3.3	Effect of $\beta$ on the pdf of a Weibull distribution.....	28
3.4	Effect of $\eta$ on the pdf of a Weibull distribution .....	28
3.5	Effect of $\eta$ and $\beta$ on the cdf of a weibull distribution .....	29
3.6	Effect of $\sigma$ on the pdf of a lognormal distribution.....	30
3.7	Effect of $\mu$ on the pdf of a lognormal distribution.....	30
3.8	Effect of $\sigma$ on the cdf of a lognormal distribution .....	31

List of figures (continued)

Figure	Page
3.9 Illustration of ecdf compared to a normal cdf.....	35
3.10 Schematic of temperature cycle profile .....	40
4.1 Electronic watt-hour meter.....	48
4.2 IR pulses emitted by meters with different Kh constants .....	49
4.3 Pulse detection circuit.....	49
4.4 Schematic of software/hardware interface.....	51
4.5 Flowchart of energy calculation algorithm .....	53
4.6 Relative sensitivity vs wavelength.....	55
4.7 Relative sensitivity vs viewing angle.....	56
4.8 Illustration of flexible gooseneck .....	57
4.9 Effect of slow sampling rate .....	58
4.10 Thermocouple illustration.....	60
4.11 Thermocouple output contaminated with noise.....	63
4.12 Schematic of the test setup.....	65
4.13 Experimental set-up showing the resistor bank, meters and transformer .....	66
4.14 The entire prototype.....	66
4.15 Envirotronics Chamber at EPRI facility .....	68
4.16 Schematic of the experiment.....	69

List of figures (continued)

Figure	Page
4.17 The actual test set-up at EPRI.....	70
4.18 Illustration of front panel and block diagram in LabVIEW .....	73
4.19 Dialog box for manufacturer's details .....	74
4.20 Main page of the DAQ software.....	76
4.21 Meter page of the DAQ software.....	80
4.22 Temperature page of the DAQ software.....	81
5.1 Calibration results for high temperature tests .....	85
6.1 Flowchart of statistical analysis for accelerated life tests.....	92
6.2 Histogram of the failure data at 110 °C .....	93
6.3 Histogram of the failure data at 130 °C .....	94
6.4 Probability plots of the failure data at 110 °C .....	96
6.5 Probability plots of the failure data at 130 °C .....	96
6.6 Lognormal characteristics of the failure data at 110 °C .....	98
6.7 Lognormal characteristics of the failure data at 110 °C .....	98
6.8 Arrhenius plot for cable insulation .....	99
6.9 Degradation data .....	102
6.10 Inverse power law plot showing stress vs life .....	103

## CHAPTER 1

### INTRODUCTION

Electricity metering is a vital part of a utility's distribution system since it is the source through which the utility gauges a consumer's utilization, and generates a monthly bill, which is the source of revenue for itself. It is important for the meters to be as accurate as possible because even the slightest under-reading of each meter can cost the utility millions, as the meters are deployed on a large-scale. On the contrary over-reading can also have an adverse effect since it could lead to legal issues and harm the reputation of a utility. Meters of different types and complexities have been used since the 1900s when electricity began to be produced and distributed commercially [1]. Most such meters in the past were of electromechanical type and consisted of windings that produced magnetic fluxes proportional to the current and voltage. These windings were aligned to rotate an aluminum disk, which in turn rotates registers for display. They worked on the working principle of an induction motor and sometimes are also called *induction disk watt-hour meters*.

With the advent of electronics, electricity meter manufacturers started to incorporate them into metering technology. The first fully electronic meters were available in 1990s but were not deployed on a large scale because they were expensive and many previously installed electromechanical meters were still within their projected lifespan. In general, utilities did not replace a meter unless it was damaged. As a result,

most electricity meters have performed for around 40 years and are now nearing the end of their lives.

Another reason for replacing old electromechanical meters has come with the passage of the United States Energy Policy Act of 2005 [2]. By the guidelines in this energy law, utilities are now encouraged to invest more resources into research pertaining to renewable energy and energy efficiency. With restrictions on construction of new thermal and nuclear plants due to environmental impact and the fact that hydro electricity is almost 100% utilized, energy efficiency has become the primary objective of the 21<sup>st</sup> century. A key feature for the success of this drive is demand response and real-time pricing. Demand response refers to load shedding or reduction of consumption of electricity (e.g. lighting, air conditioning, etc.) by the utility, with the approval of the consumer, in order save costs by keeping expensive generators offline and continue maintaining grid stability during peak demand hours. For this objective to be realized, Advanced Metering Infrastructure (AMI) needs to be in place. These meters are capable of two-way communication, remote disconnection, and real-time pricing, as well as other features.

Due to the reasons mentioned in the paragraphs above, utilities intend to spend millions of dollars in replacing the aging metering infrastructure over the next couple of years. However, with electronic meters, reliability of electronic components is a concern since they are particularly vulnerable to stresses caused by environmental conditions, voltage, current, etc.

Reliability is defined as the ability of a product to perform as designed for the expected lifespan under stated operating conditions. Reliability engineering deals with application of engineering principles and techniques to evaluate the reliability of a product and find potential areas for reliability improvement by identifying the most likely failures and then identify appropriate actions to mitigate the effects of those failures. Reliability engineering deals with the study of failure data which includes times to failure and causes of failure. This data is acquired over the years from field-testing and products returned under warranty, and in today's competitive world it is not profitable to wait for the accumulation of data from the field. Moreover, technology improvements are occurring at such a rapid pace that failures in products in the field may not occur in the new products for which the reliability needs to be predicted. In order to maintain the competitive edge, engineers need to obtain failure data quickly, and for this purpose, Accelerated Life Tests (ALT) were devised. In ALT tests, specimens of the actual product are subjected to elevated stresses such as temperature, humidity, voltage, etc. making them fail or degrade quickly. Stress levels should be chosen such that they would lie in the elevated stress zone and not lie within destruct limits in which the device would definitely sustain damage, thus providing no useful information. With data analysis, the inferences can be extrapolated to normal usage conditions. The underlying assumption of such tests is that the failure mechanism remains the same at both normal and elevated stress conditions. Reliability studies and Accelerated Life Tests have been around since 1970s, and their use was initially limited to defense and military equipment. Over the years, many manufacturers have developed reliability programs to improve the quality of

consumer products, achieve customer satisfaction, and reduce warranty costs. Many classified documents from military ALT testing have been declassified and available, along with other good resources of information on this subject [3, 4, 5].

Some of the failures that could occur in electronic systems can be attributed to evaporation of electrolyte in capacitors, solder crack formation on circuit boards, delamination of ceramic components, electromigration, and damage to microelectronic devices, etc. Although in terms of reliability, electronics have improved tremendously over the years and electronic meter manufacturers have strong reliability programs, a third party verification was requested by several utilities to gain a higher level of confidence before investing large amounts of money in replacing aging meters. As a result, this thesis was partly funded by EPRI, which in turn was funded by electric utilities, to perform a research study to assess the accuracy and life of an electronic meter in the field by utilizing accelerated life tests.

As the first phase of the project contract, an estimate of life of electronic meters in the field is required with impact of environmental conditions. Other stresses such as voltage and humidity will follow in later phases. Accelerated testing is performed on electronic meters by subjecting them to high temperatures for extended periods in an environmental chamber at an EPRI facility. The first step in assessing product life is to obtain time-to-failures. From this data, the average life of the product and other inferences can be made. Since it is not possible to observe the meters in the chamber during operation, a Data Acquisition System was built to continuously monitor the health of the meters. The fact that electronic meters have a built-in infrared LED for calibration

purposes has been exploited. Although the purpose of this LED is periodic calibration either in the lab or the field, it has been used in this project to continuously monitor the meters placed in the inaccessible environmental chamber. The software interface was programmed in LabVIEW and the system was used to count the pulse output of an electronic meter and calculate energy. When compared to a reference, the absence of pulses or drift in recorded energy, beyond a threshold, was considered a failure. The temperature of the chamber was also closely monitored with the system, since the control system of the environmental chamber may be inaccurate or distant from the meter location in the chamber. The system developed is flexible and can be adopted to be used in any future testing operations with other stresses.



## CHAPTER 2

### OVERVIEW OF METERING TECHNOLOGY

#### Introduction

Revenue metering refers to monitoring the usage of a resource such as electricity, water or natural gas for the purpose of generating revenue. Electricity is one of the more important revenue generating resources and monitoring it can be more complicated than others. This chapter discusses the fundamental principles of electricity metering and the latest trends in this area, and is important since it compares and contrasts traditional methods and new electronic meters. It also gives insight into the functionality, construction, and calibration of these new electronic meters, which can be useful later chapters.

#### Electromechanical meters

Traditionally electricity has been measured by the use of electromechanical meters. Such meters have a proven track record of lasting over 40 years in the field, and are not prone to catastrophic failures. Although they have other problems associated with them, they generally perform reliably requiring only a calibration check once every 5-7 years. An electromechanical meter works on the principle of operation of an induction motor. It contains a rotating aluminum disk in which the angular speed of this disk is proportional to the voltage applied and the current flowing through the windings that produce magnetic flux. Since it is based on this principle, the power factor is

automatically accounted for and the disk spins at a rate proportional to the true power ( $S$ ). The disk is then attached to a register through an appropriate gearing ratio, to obtain the actual kilowatt hours seen by the meter.



Figure 2.1 Front view of an electromechanical watt-hour meter  
(Source: [www.tdsurplus.com](http://www.tdsurplus.com))

Since the meter is based on the principles of an induction motor, the disk behaves like a squirrel cage rotor where torque is produced by the induced eddy currents due to the disk's position in the time-varying magnetic field. The EMF is created by the current carrying coils in conjunction with the voltage coils. In order to ensure that the measurement is accurate, the torque (and hence the speed) should be at the maximum

possible value when the system is at unity power factor. To ensure this, a lag coil is used on the voltage pole so that the current in the voltage coil lags the voltage by  $90^\circ$ . Current in the lag coil, and hence the angle between voltage and current, can be varied using the lag resistor. This is shown in the Figure 2.2. The permanent magnets are in place to reduce the speed of spinning since there is negligible friction.

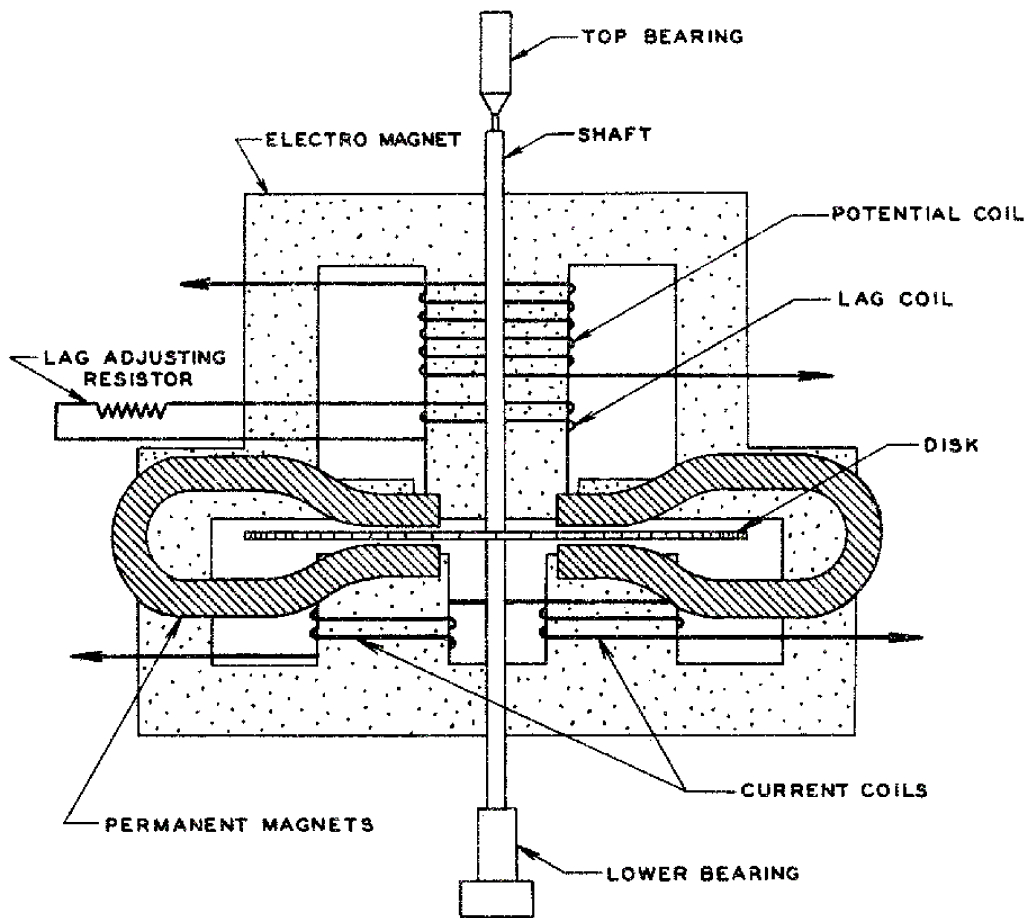
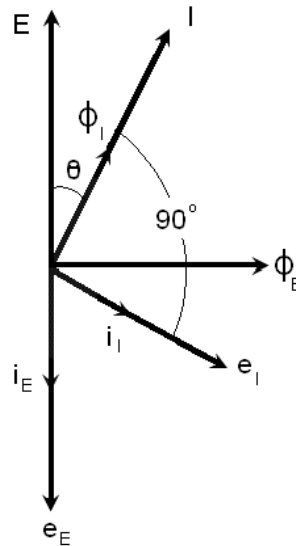


Figure 2.2 Components of a single-phase induction watt-hour meter [6]

Multi-element meters consist of additional elements stacked vertically, with two or more disks on the same shaft. These meters may have more than one electromagnet system acting on the same disk.



Where

$E$  = Voltage on potential coil

$I$  = Current through current coil

$\phi_E$  = Potential coil flux

$\phi_I$  = Current coil flux

$e_E$  = Disc voltage induced by  $\phi_E$

$e_I$  = Disc voltage induced by  $\phi_I$

$i_E$  = Disc current induced by  $e_E$

$i_I$  = Disc current induced by  $e_I$

Figure 2.3 Vector diagram of the operating quantities in a watt-hour meter [6]

The vector diagram above depicts the quantities involved in the operation of a basic single-phase electromechanical meter. Torque is produced due to the interaction between  $i_I$  with  $\phi_E$  and  $i_E$  with  $\phi_I$ .

Every manufacturer's meter construction is different. Moreover, they are deployed in different circuits that have different ranges of load currents and voltages. Therefore, knowledge of meter constants is required for purchasing the appropriate

meter, and to also check the accuracy of kilowatt-hours as read from the register. These constants are provided on the name-plate details of the meter and some of them can be verified by visual inspection.

Watt-hour constant (Kh): - The watt-hour constant is the registration of one revolution of the rotating disk element expressed in watt-hours. The watt-hour constant is also sometimes called the disk constant.

Gear ratio (Rg): - The gear ratio of a meter is the number of revolutions of the rotating disk element for one revolution of the first dial pointer.

Register ratio (Rr): - The register ratio of a meter is the number of revolutions of the wheel meshing with the worm or pinion on the rotating disk element, for one revolution of the first dial pointer.

Register constant (Kr): - The register constant is a factor by which the register reading is multiplied to ascertain the number of kilowatt-hours recorded by the meter. The register constant is also sometimes called the dial constant or multiplier.

Some of the common causes of errors are listed below. These do not include inherent causes such as temperature, humidity, frequency, etc.

- Dirt (on the disk and the air gap)
- External magnetic fields
- Broken jewels
- Dirty and improperly adjusted bearings
- Vibration
- Creep

- Overload or internal short circuit
- Presence of harmonics

Sometimes the disk of a meter may move, either forward or backward, when all loads are disconnected. This is called creep error. A meter in service is considered to creep when, with all load wires disconnected and test voltage applied, the moving element makes one revolution in ten minutes or less. Creep is generally minimized by punching holes or slots in the disk so that it gets locked under the field of the voltage pole when the meter is unloaded.

Electromechanical meters also cannot account for harmonics and hence will record watt-hours incorrectly. This is not an error caused by meter defects but by the quality of the power being supplied and power factor of the load. However, it is an important error-causing source. This error is minimized or completely removed in electronic meters by the addition of filters in their internal circuitry.

### Electronic meters

Until the 1970's all the meter manufacturers produced electromechanical meters. In the 1970s, the first meters were installed with electronic registers [2]. By the mid-1980s, the first hybrid meter was available in the market with electronic registers mounted on induction type watt-hour meters [2]. Tremendous development in electronics led the path to a completely electronic meter by early 1990s [2]. Since then, electronic meters have improved in their functionality and reliability.



Figure 2.4 Front view of an electronic watt-hour meter  
(Source: GE I-210 User Manual)

The working of electronic meters can be sub-divided into functional blocks. The functional block diagram along with the discrete electronic components that electronic meters comprise of are listed below and depicted in Figure 2.5

Power Supply: This module generally consists of an AC to DC converter which supplies the electronic components with digital voltage (0-5 V DC). Different manufacturers used different topologies but the fundamental components may include control transformer, semiconductor diodes, resistors and capacitors.

Signal Conditioning: It comprises of current and voltage sensors along with some filters. Components used are, metal oxide varistors (MOVs), resistors, capacitors and sometimes ferrite cores (inductors).

Analog to Digital Converter: Converts the voltage and current signals into digital data. The resolution of the ADC is an important factor in determining the accuracy of the meter. It is generally in the form of an IC and may be included in the processor chip.

Digital Signal Processor: Processes current and voltage signals to calculate power and deduce kilowatt-hours. It is a semiconductor device, and is generally the largest one on the circuit board.

Calibration LED: In order to test an electronic meter for accuracy of the display, a calibration LED is provided as a standard requirement that emits infrared pulses proportional to the energy recorded.

LCD display: The display shows the energy accumulated. Advanced meters can show other parameters too such as reactive power, harmonic content, etc.

AMR infrastructure (optional): Advanced Meter Reading infrastructure is a set of communication components that are begin introduced in the new meters. They can



provide data to the revenue collection center without human involvement. They can also be used for remote disconnect. This topic will be dealt in detail later.

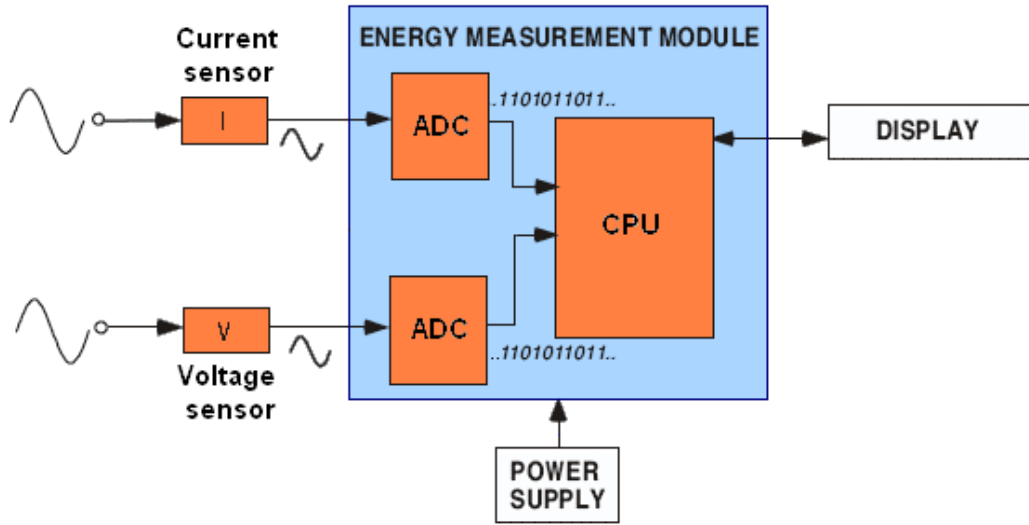


Figure 2.5 Schematic of an electronic watt-hour meter [7]



Figure 2.6 Internal components of an electronic watt-hour meter (Landis + Gyr Focus<sup>®</sup> meter)

## Advanced Metering Infrastructure

### *Automated Meter Reading (AMR)*

Traditionally, meter readings were taken manually since they did not possess any communication capabilities. A representative from the utility had to drive through a community and manually read each meter. Gradually, communication features were introduced for cost benefits. The first communication technique was to run a wire from the meter location up to the measuring station. These were called KYZ connections and transmitted pulses corresponding to energy consumed. At present, a variety of communication protocols and technologies are available so that meters can be remotely read. Such communication features can provide additional information such as load profile of individual users, communities, etc. and has greatly helped in research and improvement of electrical services. AMR is the name given to the collective technology of communication networks, software and other components used to collect data from revenue meters automatically and transferring it to processing centers through a communication protocol. Communication protocols may include radio frequency, Wi-Fi, power line carrier, etc. AMR meters have been deployed in large numbers in other countries such as Italy, Sweden, etc. Their deployment has been rather slow in the US, and is expected to pick-up in the coming years.

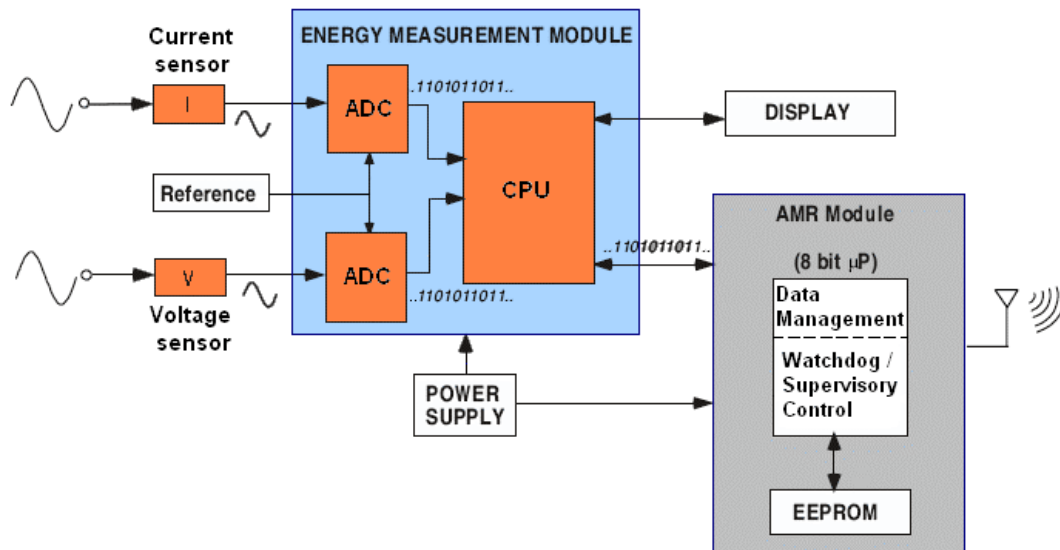


Figure 2.7 Schematic of an electronic watt-hour meter with AMR [7]

### *Advanced Metering Infrastructure (AMI)*

In AMR, only one-way communication is present, whereas, in Advanced Metering Infrastructure (AMI), two-way communication with the meter is possible. They can be controlled remotely, are able to be programmed to collect data periodically, and allow for remote disconnection in case of required peak shaving or default of payments. AMI systems are new and with the present trend highly focused on energy efficiency and demand response, AMI systems are to be deployed on a large scale in the US during the next few years. This infrastructure includes hardware, software, and communication protocols. Since the technology is new, it is rather expensive and reliability has yet to be assessed.

### Meter Testing and Calibration

The term meter calibration means determination of accuracy in energy registration of a watt-hour meter. In measuring accuracy of a meter, the term percentage registration is used rather than percentage error. It is defined as

$$\% \text{ registration} = \frac{\text{actual registration}}{\text{true registration}} \times 100 \quad (2.1)$$

In electromechanical meters, a direct correlation exists between the speed of spinning disk and the register (display). In electronic meters, a separate circuit is internally present, which produces infrared pulses, using an infrared LED, proportional to the energy consumed as calculated by the Digital Signal Processor. These sources are used to independently measure the accuracy of a meter. Commercial meter testing and calibration devices are available as shown in Figure 2.8. They contain a voltage source and connected to a known load to draw constant current without voltage fluctuations. The energy meter is connected in series with the load, and energy registration on the meter is noted over a time interval. By knowing the true energy dissipated, and comparing it to that read by the meter, percentage registration can be calculated as per the Equation 2.1. The limits of error are specified by different standards such as ANSI and IEC [6, 8].



Figure 2.8 UTEC 5600 Universal Calibration device  
(Source: [www.radianresearch.com](http://www.radianresearch.com))

WATT-HOUR AND DEMAND METER TEST REPORT									
LOCATION Rainbow #2		CIRCUIT Montana Power Company				DATE 5-5-71			
WATT-HOUR METER			DEMAND METER		METER READINGS			TIME	
Manufacturer	General Elec.				As found				
Serial No.	1269039				Dial 0325.6			8:30 a.m.	
Type	DG2		Recording		Demand			p.m.	
Style/Model	8WDG2JAS190				Revolutions 1			Seconds 117	
Class					As left				
Multiplier	10,000		80,000		Dial 0326.6			11:30 a.m.	
Primary $K_h$			KW Full Scale 78,500		Demand			p.m.	
Secondary $K_h$	0.9		Dem. Interval 30		Revolutions 1			Seconds 52	
Amps	2.5		Chart No. 6724A		DEMAND METER TESTS				
Volts	120		Contact Device D13		AS FOUND			AS LEFT	
Elements	2		Gear Ratio 10/9		Revolutions 100				
Reg. Ratio	13-8/9		1 rev (8 impulses) =		Demand 0.18				
1st Reduction	100		111-1/9 meter revs		Revolutions				
Detent	Yes				Demand				
C.T. Ratio	80/1		P.T. Ratio 1,000/1		% Accuracy 100.0				
STANDARD DATA			Correction		VOLTAGE READINGS			PHASE ANGLE	
Manufacturer	Model		Serial Number		PHASE		VOLTS		I <sub>1</sub> I <sub>2</sub> I <sub>3</sub>
GE	IB-10		6009523		1-2		(Load too small)		
CURRENT READINGS					2-3				
PHASE	PRIMARY	SECONDARY	% BURDEN		3-1		111		
A	55	0.7	56		1-N		110		
B	60				2-N				
C	60	0.74	59		3-N		110		
CONDITION OF METER									
General OK					Register Cleaned				
Demand Mechanism OK					Upper Bearing Replaced				
Jewels & Ball Cleaned - replaced					Rotation of individual Elements OK				
Potential Creep No									
METER REGISTRATION									
TEST	STANDARD		METER		AS FOUND			AS LEFT	
	$K_h$	Amps	Elements	Revs.	Standard	% Registration	Standard	% Registration	
Full Load Series, 1.0 P.F.	.6	2.5	2	20	15.00	100.0	14.97	100.2	
Light Load Series, 1.0 P.F.	.12	0.25		4	14.92	100.53	14.98	100.13	
Power Factor Series, .5 P.F.	.6	2.5		20	14.98	100.13	14.97	100.2	
Full Load Individual Elements at 1.0 P.F.			Upper		5	7.47	100.4	7.46	100.53
			Lower		5	7.53	99.6	7.48	100.27
Light Load Individual Elements at 1.0 P.F.			Upper		1	7.50	100.0	7.47	100.4
			Lower		1	7.52	99.73	7.49	100.13
Power Factor Individual Elements at .5 P.F.			Upper		5	7.50	100.0	7.47	100.4
			Lower		5	7.45	100.67	7.47	100.4
Dial Adjustment = $0.9 \times 0.83 \times 60 \times 3 \times 8$					0325.6		Dial Reading As Found		
					1.0		+Dial Adjustment		
					0326.6		Dial Reading As Left		
Remarks									
Tested by Sam Rapos, USBR					Assisted by				

Figure 2.9 Sample Utility meter calibration report [6]

## CHAPTER 3

### RELIABILITY AND ACCELERATED LIFE TESTING

#### Introduction

Reliability is defined as the ability of a product to function without failures under stated conditions and for a declared period of time. The conditions under which the product is to operate are called usage conditions and the time for which the product is to function without defects is called product life-time. The following are a few reasons why reliability studies needs to be carried out:

- Predict the life-time of a product
- Determine optimal burn-in time
- Research and development of the product (materials used, design, etc.)
- Minimize production and life-cycle costs.
- Determine optimal usage conditions.
- Optimize warranty policies

Reliability is expressed in terms of probability and can be interpreted as the probability of a product surviving after a time ' $t$ '. It can be obtained by subtracting the cumulative density function (CDF) from 100% failure probability (or 1). Mathematically, reliability can be expressed as:

$$R(t) = 1 - F(t) \tag{3.1}$$

where  $F(t)$  is the cumulative probability of failure.

There are certain organizations that provide qualification standards and specifications (such as IEC, ANSI, etc.) for the performance of a product. However, qualification standards and requirements are good only to confirm that the given product is qualified to function in a particular range of operating parameters. In some cases, especially for new products and new technologies when no prior experience has been accumulated, the general qualification standards based on the previous experience of older products might be too stringent. An unreasonable qualification test, that does not reflect the actual field conditions, might result in a rejection of a good product which might perform properly for a long time. On the other hand, the qualification specifications might not be severe enough for particular use conditions, and a product without a high enough reliability level may pass the test specifications. Since qualification tests are not destructive, they do not provide the required information about the reliability of the product, i.e., the time-to failure data under the given conditions of operation.

It is clear that to predict and optimize life-cycle characteristics of a product, reliability testing needs to be carried out. The problem involved in implementing reliability engineering techniques is that it requires time-to-failure data of the product. Time-to-failure data is a collection that includes failure times, of a considerable number of products, since beginning of operation and causes of those failures, and is generally available from testing in the field or products returned through a manufacturer's warranty program. From this data important predictions can be made regarding the life and quality of the products. This data is not easily available because of the long lifetimes of today's



products, and moreover laboratory testing with usage conditions will also does not yield any failures. In order to maintain the competitive edge, a manufacturer has to reduce the time gap between R&D stage and market release so that products reach the market before their competitor's products and this effectively reduces testing time.

This problem is overcome by deliberately operating the product at an elevated stress condition so that failures are induced quickly. Reliability analysis can then be performed using the failures at this elevated condition, and the results can be mapped to usage levels of stress. This entire technique is called Accelerated Life Testing Analysis (ALT). ALTs deal with two areas of reliability engineering- physics (failure mechanisms) and statistics. Failures that occur in products generally follow a pattern, for example, a capacitor may fail because of evaporation of its electrolyte which in turn depends the ambient temperature. By increasing the ambient temperature, we can cause the capacitor to fail faster than it would in normal conditions. The determination of cause-effect phenomena, due to which the failure occurs, is called a failure mechanism. Every kind of applied stress produces different phenomena and the most common accelerated stress conditions are:

- High and low temperature
- Temperature cycling and thermal shock
- Mechanical shock and fatigue tests
- Vibration tests
- Voltage extremes
- High humidity

Sometimes, a combination of two or more stresses is applied to simulate real-life operating conditions. The underlying assumption, while conducting ALTs, is that the failure mechanism remains the same at the design stress as well as the elevated stress. A list of failure mechanisms and their related stresses are available in literature [9]. Some of the failures and the stresses that cause them can be found in Table 3.1.

Table 3.1 Failure mechanisms and related stresses [9]

<b>Failure Mechanisms</b>	<b>Accelerating Stresses</b>
Corrosion	Corrosive atmosphere, temperature, relative humidity
Creep and stress relaxation (static, cyclic)	Mechanical stress, temperature
Delamination	Temperature cycling, humidity, frequency
Diffusion	Temperature, concentration gradient
Electromigration and thermomigration (forced diffusion due to electric potential or thermal gradients)	Current density, temperature
Fatigue and brittle crack initiation & propagation	Mechanical stress range, cyclic temperature range, frequency
Radiation damage	Intensity of radiation, total dose of radiation
Stress corrosion cracking	Mechanical stress, temperature, humidity

### Data Types

Classification of data is very important since statistical models rely extensively on the time-to-failure data, and the accuracy of the results depends on the accuracy and

completeness of data. Different statistical approaches have to be undertaken for different types of data. Data, in general, can be classified into two types as discussed:

Complete data: A data set is known to be complete when the time-to-failure of each and every unit in the sample is known.

Censored data: In many cases, when accelerated testing is done, all units in the sample may not fail or the exact times-to-failure may be unknown. This type of data is called censored data. Censored data can be sub-classified into:

*Type I:* In this type, the exact failure times  $t_1, t_2 \dots t_r$  are known and there are  $(n - r)$  units that survive the entire  $t$ -hour test without failing. This type of censoring is also called *right censored* or *time censored* data since the times of failure to the right (i.e. larger than  $t$ ) are missing.

*Type II:* In this type, the number of failures to be observed is decided in advance and testing is stopped once the target is achieved. The exact failure times  $t_1, t_2, \dots, t_r (t=t_r)$  are observed and there are  $(n - r)$  units that do not fail when testing is aborted. This type of data is also called *failure censored* data and is generally avoided because failures may occur after very long periods which may not be economical.

*Interval Censored:* Sometimes, the exact failure times are not known and only the interval of time in which the failure occurred is available. This may happen when the

testing facility is not accessible continuously. Examples may include thermal chamber or radiation chamber. This kind of data is called *interval censored* data.

### Statistical Analysis

The objective of ALT is to predict the “mean life” at normal operating conditions. Once the failure mechanism has been identified and test plan designed, testing is done and failure data is recorded. This is followed by statistical analysis to determine required parameters. This process can be briefly subdivided into the following steps and each of these is explained in detail:

1. Choice of distribution
2. Parameter estimation
3. Goodness-of-fit testing
4. Models for accelerated life testing

#### *Choice of distribution*

The first step in statistical analysis is to fit the data onto a probability distribution. From this distribution, the probability of failure of a unit at any given instant of time can be calculated. Experience shows that most testing and laboratory data can usually be appropriately fitted onto one of the three distributions described below [3, 5]. However other distributions may also be applicable and depends on the data obtained from testing.

Exponential: The exponential distribution is a commonly used distribution in reliability engineering. The exponential distribution is used to model the behavior of units that have a constant failure rate. Mathematically it is a simple distribution with only one parameter to determine and hence it is used widely, even in inappropriate situations [3]. Thus care should be taken to check if the data actually could be modeled using an exponential distribution or not. The probability density function is given by the equation:

$$f(t) = \lambda e^{-\lambda t} \quad (3.2)$$

where  $\lambda$  is the constant rate of failure

$t$  is the time-to-failure from data observed

Figures 3.1 and 3.2 show the effect of change in  $\lambda$  on the probability density function (pdf) and cumulative distribution function (cdf).

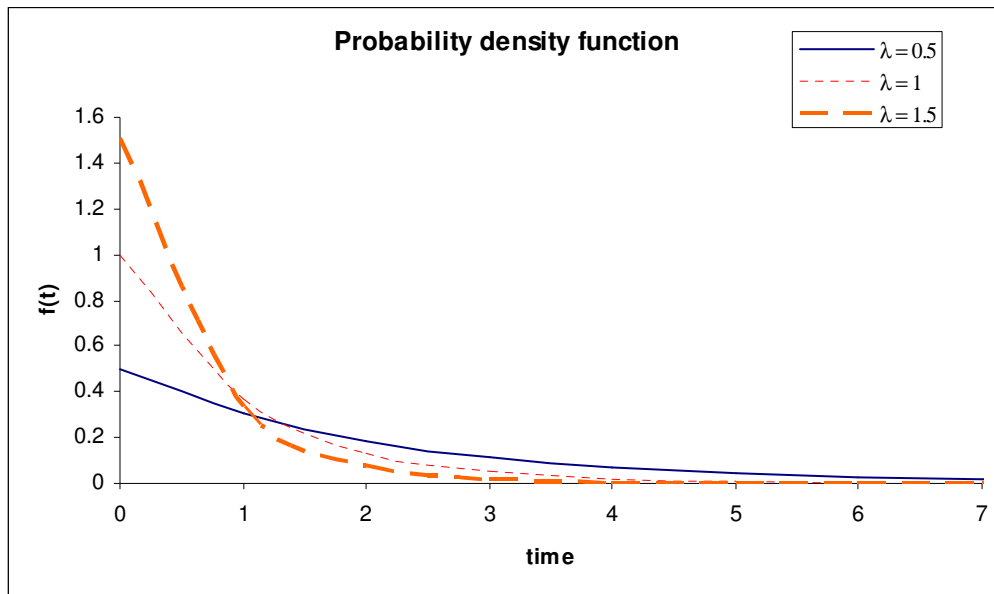


Figure 3.1 Effect of  $\lambda$  on the pdf of an exponential distribution

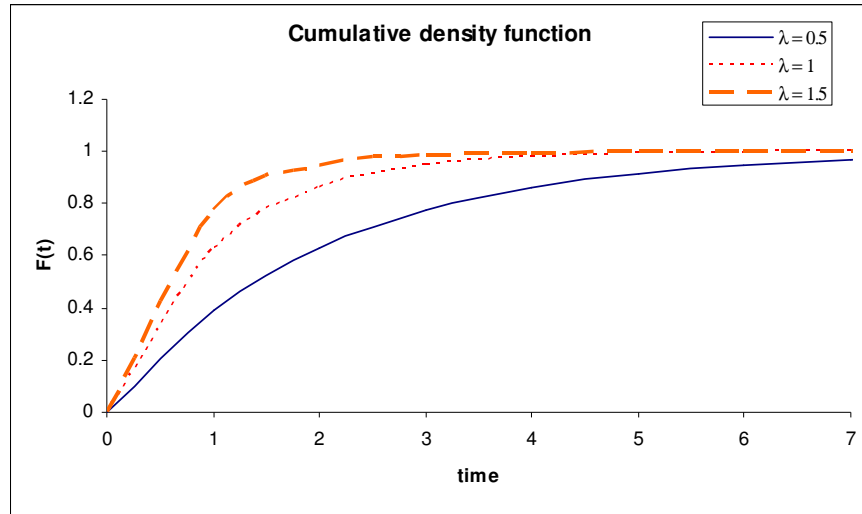


Figure 3.2 Effect of  $\lambda$  on the cdf of an exponential distribution

Weibull: The Weibull distribution is one of the most widely used distributions in reliability engineering. It is very useful since it is flexible and can take the shapes of different distributions to fit various kinds of data. This is accomplished by varying the shape parameter  $\beta$ . The probability density function is given by the equation:

$$f(t) = \frac{\beta}{\eta} \left( \frac{t}{\eta} \right)^{\beta-1} e^{-\left( \frac{t}{\eta} \right)^\beta} \quad (3.3)$$

where  $\beta$  is the shape parameter and  $\eta$  is the scale parameter

The advantage of Weibull distribution is that it is versatile. Change in parameters  $\beta$  and  $\eta$  makes the distribution change in shape and this effect is depicted in the graphs below. When  $\beta = 1$ , Weibull distribution takes the shape of an exponential distribution.

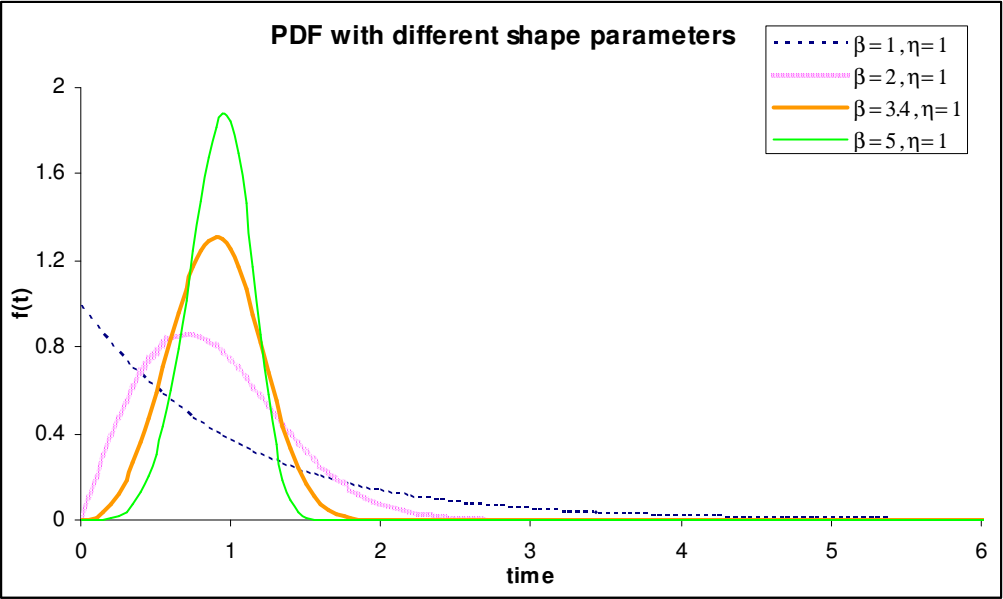


Figure 3.3 Effect of  $\beta$  on the pdf of a Weibull distribution

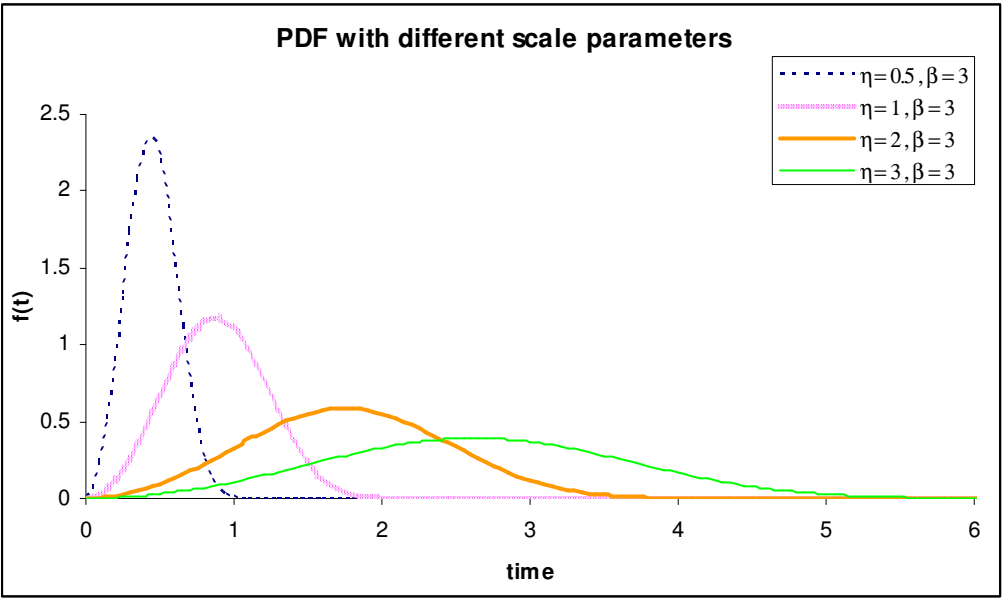


Figure 3.4 Effect of  $\eta$  on the pdf of a Weibull distribution

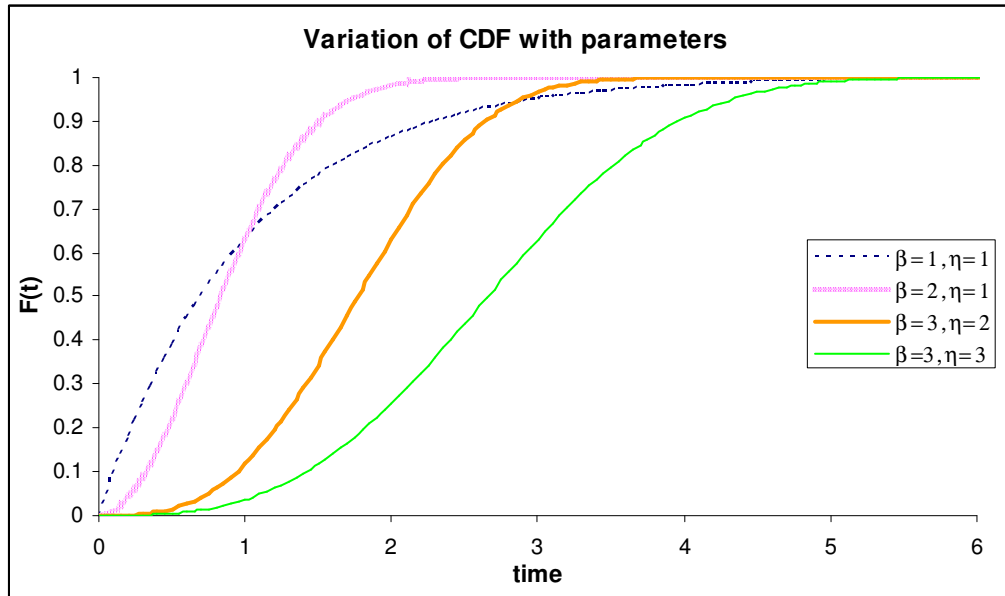


Figure 3.5 Effect of  $\eta$  and  $\beta$  on the cdf of a weibull distribution

Lognormal: The lognormal distribution is another distribution with widespread applications. It is generally used to model the life when the failure mode is of fatigue-stress nature. The probability density function of a lognormal distribution is:

$$f(t) = \frac{1}{t\sigma\sqrt{2\pi}} e^{-\frac{1}{2}\left(\frac{\ln t - \mu}{\sigma}\right)^2} \quad (3.4)$$

where  $t$  is the time-to-failure

$\mu$  is the mean of the natural logarithms of the times-to-failure

$\sigma$  is the standard deviation of the natural logarithms of the times-to-failure



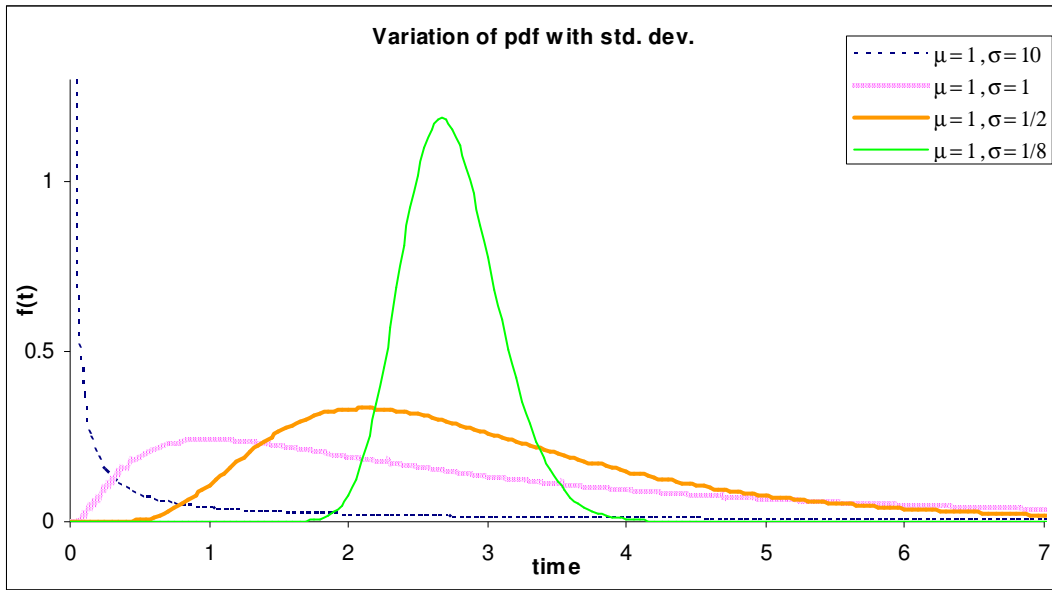


Figure 3.6 Effect of  $\sigma$  on the pdf of a lognormal distribution

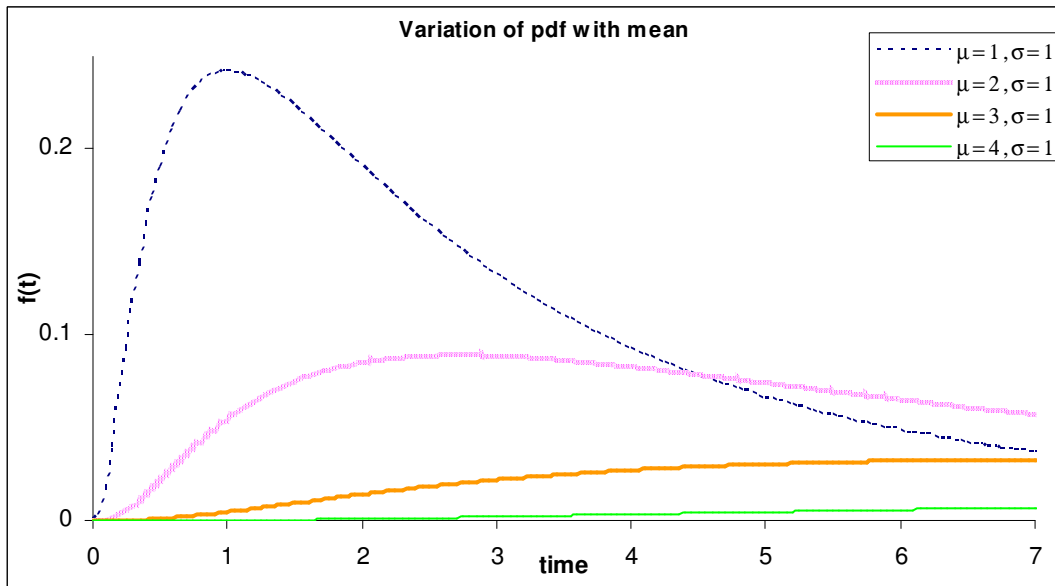


Figure 3.7 Effect of  $\mu$  on the pdf of a lognormal distribution

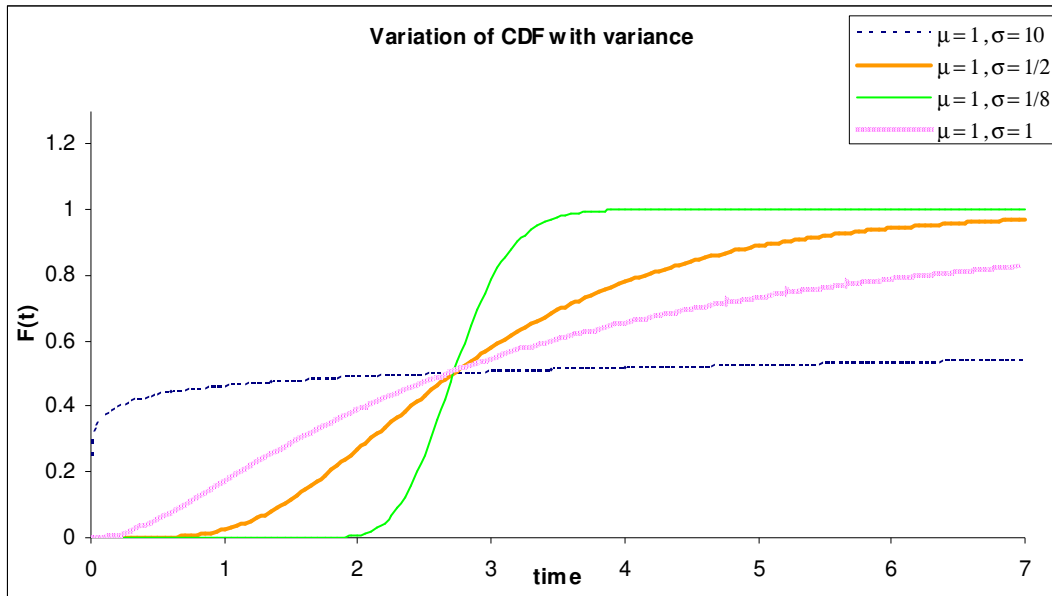


Figure 3.8 Effect of  $\sigma$  on the cdf of a lognormal distribution

### *Parameter estimation techniques*

In the distributions described above, it is essential to get accurate parameters to describe the system closely. Some of the methods used to estimate the parameters are briefly described below:

Least Squares Method (LSM): The least squares estimation is a technique that determines the unknown quantities by minimizing the square of the residuals (i.e. the difference between predicted value and the observed value). Least squares estimation can be performed for linear as well as for non-linear functions and information on this topic is available at [8].

Mathematically, the least squares criterion that is minimized to determine the parameters can be expressed as:

$$S(A_0, A_1, \dots, A_N) = \sum_{i=1}^n [y_i - f(x_i, A_0, A_1, \dots, A_N)]^2 \quad (3.5)$$

where  $A_0, A_1, \dots, A_N$  are the parameters of the function that need to be determined

$(x_i, y_i)$  where  $i=1,2,3,\dots,n$  are the set of observations

The disadvantages of least square estimation are:

- LSM for a non-linear function does not have any closed loop solution and must be solved iteratively and hence requires more computational effort.
- LSM is not robust and estimates can be highly biased if we have censored data. In such a situation, Maximum Likelihood Estimation (MLE) is preferred.

Maximum Likelihood Estimation (MLE): Maximum likelihood estimation is a powerful statistical method that is used to determine the parameters of a mathematical model which represents observed data. It can be used for both complete as well as censored data. If  $t$  is a continuous random variable with PDF as  $f(x; A_0, A_1, A_2, \dots, A_k)$  where  $A_0, A_1, A_2, \dots, A_k$  are the constant parameters of the PDF that need to be estimated and an experiment is conducted where  $N$  independent observations are made, then likelihood function (assuming we have complete data) is defined as:

$$L(x_1, x_2, x_3, \dots, x_N | A_0, A_1, A_2, \dots, A_k) = \prod_{i=1}^N f(x_i; A_0, A_1, A_2, \dots, A_k) \quad (3.6)$$

The logarithmic likelihood function is derived by taking the natural logarithm of Equation 3.6 and is shown below:

$$\Lambda = \ln L = \sum_{i=1}^N \ln f(x_i; A_0, A_1, A_2, \dots, A_k) \quad (3.7)$$

The maximum likelihood estimators of the parameters  $A_0, A_1, A_2, \dots, A_k$  are then obtained by maximizing  $L$  or  $\Lambda$ . This is done by obtaining the partial derivatives with respect to each of the parameters and equating to zero. It is easier to work with the log likelihood function and is more frequently used, since a product of terms is transformed into a sum, and the derivative is relatively easier to calculate.

$$\frac{\partial(\Lambda)}{\partial A_i} = 0 \text{ where } i = 1, 2, 3, \dots, N \quad (3.8)$$

The disadvantage of maximum likelihood estimators is that the estimates are biased if the sample is small. Depending upon the data available, both methods should be tried and more conservative values should be taken for accurate results.

#### *Goodness-of-fit tests*

When the failure data is fit to a population distribution, it must be tested to check whether the distribution actually models the underlying data appropriately. Three popular tests that are used to assess the goodness-of-fit are:

Chi-Squared test: The Chi-Squared test can be applied to any univariate (only one dependent variable) distribution for which a CDF can be determined. The Chi-Squared

test is applied to binned data (i.e., data put into discrete bins) and, the size of the bin chosen is critical for the accuracy of the statistics. Another disadvantage of this test is that it requires a considerably sized data set for the chi-square approximation to be valid. To perform this test, data is divided into  $k$  bins and the test statistic is calculated as:

$$\chi^2 = \sum_{i=1}^k \frac{(O_i - E_i)^2}{E_i} \quad (3.9)$$

where  $O_i$  is the observed frequency

$E_i$  is the expected frequency

The expected frequency is calculated by the equation:

$$E_i = N(F(Y_U) - F(Y_L)) \quad (3.10)$$

where  $F$  is the CDF of the distribution that is being tested

$Y_U$  is the upper limit for class  $i$

$Y_L$  is the lower limit for class  $i$

This test statistic approximately follows the chi-square distribution with  $k-c$  degrees of freedom and significance level of  $\alpha$  where  $k$  is the number of non empty bins and  $c$  is the number of parameters plus one.

The hypothesis that a set of data is from a particular distribution is rejected if

$$\chi^2 > \chi^2_{(\alpha, k-c)} \quad (3.11)$$

where  $\chi^2_{(\alpha, k-c)}$  is the chi-squared distribution value with  $(k-c)$  degrees of freedom and  $\alpha$  significance level.

Kolmogorov-Smirnov (K-S) test: The Kolmogorov-Smirnov test is based on the empirical density function (ECDF). If we are given  $N$  ordered data points  $T_1, T_2, T_3, \dots, T_N$ , the ECDF is defined as:

$$E_N = \frac{n(i)}{N} \quad (3.12)$$

Where  $n(i)$  is the number of points less than  $T_i$

It should be noted that  $T_i$  are arranged in an increasing order. This is depicted in the graph below:

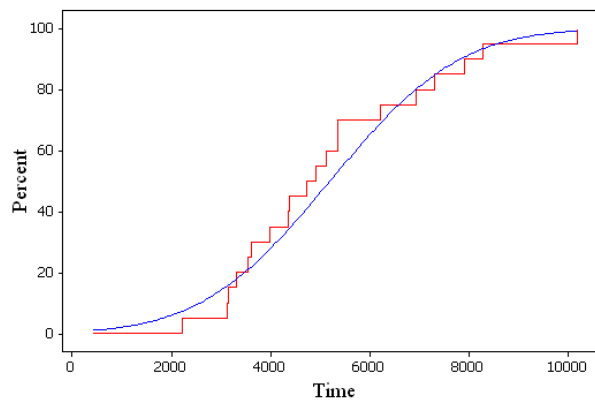


Figure 3.9 Illustration of ecdf compared to a normal cdf

The K-S test is based on the maximum distance between these two curves. The equation for the test statistic  $D$  is given by:

$$D = \max_{1 \leq i \leq N} \left( F(T_i) - \frac{i-1}{N}, \frac{i}{N} - F(T_i) \right) \quad (3.13)$$

where  $F$  is the cdf of the underlying distribution of the sample.

The hypothesis that the data represents the underlying distribution is rejected if the test statistic  $D$  is greater than the critical value obtained from a table in [8]. There are several variations of these tables in the literature that use different scaling for the K-S test statistic and critical regions. These alternative formulations must be equivalent, but it is necessary to ensure that the test statistic is calculated in a way that is consistent with how the critical values were tabulated.

The advantages of the K-S test are:

- It does not depend on the underlying distribution
- It is an exact test that does not depend on the sample size

The disadvantages of the K-S test are:

- It only applies to continuous distributions.
- It tends to be more sensitive at the center of the distribution than the tails

Anderson-Darling test: The Anderson-Darling is similar to the Kolmogorov-Smirnov (K-S) test but its critical values are distribution specific. It is more effective than the K-S test but it has the limitation of being available only for few distributions. It is generally

advisable to be used with sample sizes of  $n \leq 25$ . When tested for large samples, even small abnormalities cause the failure of the test.

The equation for the test statistic  $A$  to check if the data is from a distribution with cdf ' $F$ ' is:

$$A^2 = -N - S \quad (3.14)$$

where  $S = \sum_{k=1}^N \frac{2k-1}{N} [\ln F(T_k) + \ln(1 - F(T_{N+1-k}))]$

If the statistic  $A$  is greater than the critical value, obtained from references [8], then the hypothesis of that particular type of distribution is rejected.

#### *Models for accelerated life testing*

These models are used for relating the failure data at accelerated conditions to normal stress conditions. They may be physics based or parametric. The underlying assumption when using any of these models is that the components operating under normal conditions experience the same failure mechanism as those occurring at the accelerated stress conditions. It is assumed that the time-scale transformation or acceleration factor  $A_F$  is constant and hence implies linear acceleration.

Arrhenius model: Temperature is commonly used as an environmental stress for testing of electronic devices. This is generally modeled using the Arrhenius reaction rate equation given by:



$$r = Ae^{-\frac{E_A}{kT}} \quad (3.15)$$

where  $r$  is the speed of reaction

$A$  is an unknown non-thermal constant

$E_A$  is the activation energy (eV)

$k$  is Boltzman's constant ( $8.617385 \times 10^{-5}$  eV / K)

$T$  is the absolute temperature (Kelvin)

It is assumed that the life of a device is inversely proportional to the rate of the reaction and hence can be written as:

$$L = \frac{1}{r} = Ae^{\frac{E_A}{kT}} \quad (3.16)$$

The relationship between life at normal operating temperature  $L_o$  and that at elevated stress level  $L_s$  can be written as

$$L_o = L_s e^{\frac{E_A}{k} \left( \frac{1}{T_o} - \frac{1}{T_s} \right)} \quad (3.17)$$

The life at elevated stress condition can be obtained from the underlying distribution as shown in the previous sections. Using Equation 3.17 above, life at normal operating conditions can be predicted.

Eyring model: The Eyring model is similar to the Arrhenius model. However, the Eyring model can also be used to model data from other single or multiple stress conditions such as electric field, mechanical, etc. The Eyring model for temperature acceleration is:

$$L = \frac{1}{T} e^{\frac{\beta}{T} - \alpha} \quad (3.18)$$

where  $\alpha$  and  $\beta$  are constants determined from test data

$L$  is mean life

$T$  is the absolute temperature (Kelvin)

The general form of the Eyring model is:

$$L_S = \left( \frac{\alpha}{T_S} \right) e^{\frac{E_A}{kT_S}} e^{S \left( \beta + \frac{\gamma}{T_S} \right)} \quad (3.19)$$

where  $\alpha$ ,  $\beta$  and  $\gamma$  are constants that need to be determined

$E_A$  is the activation energy (eV)

$k$  is Boltzman's constant ( $8.617385 \times 10^{-5}$  eV / K)

$T$  is the absolute temperature (Kelvin)

$S$  is the applied physical stress

Coffin-Manson Model: This model is used to test electronic devices when the stress is a thermal cycle. The failure mechanism is thermal cracking. The temperature cycle profile can be characterized by

- High extreme temperature ( $T_{max}$ ),
- Low extreme temperature ( $T_{min}$ ),
- Temperature change  $\Delta T$ ,  $\Delta T = T_{max} - T_{min}$
- Ramp rates,
- Dwell times at extreme temperatures

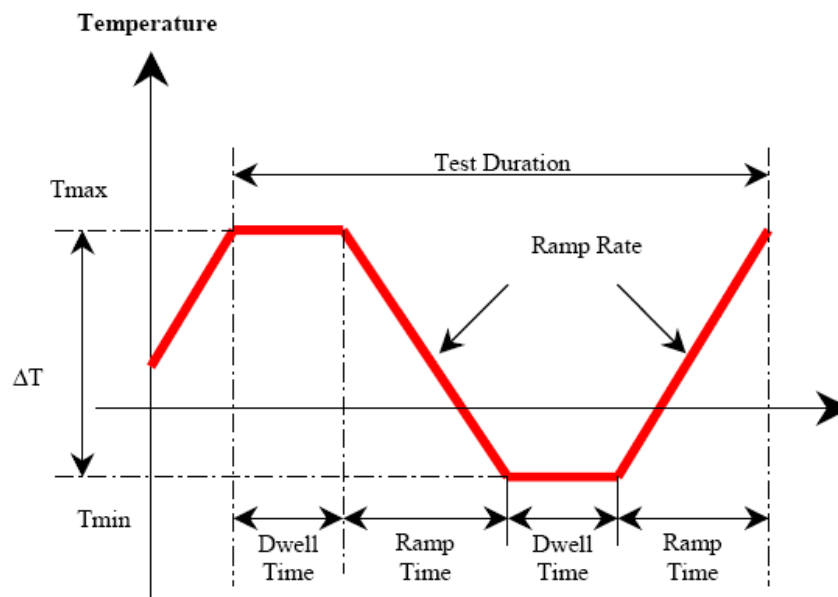


Figure 3.10 Schematic of temperature cycle profile [11]

The Coffin-Manson model considers 3 factors: maximum temperature,  $T_{max}$ , temperature change,  $\Delta T$ , and cycling frequency,  $f$ .

The equation of the model is:

$$N = A f^{-a} \Delta T^{-b} G(T_{\max}) \quad (3.20)$$

where  $N$  is the number of cycles to fail

$f$  is the cycling frequency

$\Delta T$  is the temperature range during a cycle

$A$  is an unknown constant coefficient

$a$  is the cycling frequency exponent, a typical value is around -1/3

$b$  is the temperature range exponent, a typical value is around 2

$G(T_{\max})$  is  $e^{\frac{E_A}{k T_{\max}}}$  is an Arrhenius term evaluated at the maximum temperature,

$T_{\max}$ , reached in each cycle

$k$  is Boltzman's constant  $8.623 \times 10^{-5}$  eV/K

$E_A$  is the Activation Energy

The drawback in this model is that it cannot tell the difference between dwell time and ramp time. Dwell time and ramp rate are critical factors. Dwell time is important for creep development, especially at high temperature. The ramp rate is the key difference between temperature cycle and thermal shock. Thermal shock has a much higher ramp rate than temperature cycle and causes more damage.

## Test plans

Accelerated testing is an expensive process. It involves a lot of time and money. Careless or improperly planned tests will be costly both in time and money and will not yield any useful data. On the other hand, carefully planned tests are more likely to reduce time, yield better results, and reduce the number of specimens to be tested. Detailed information on planning of tests is available in literature [3, 5]. Test plan devised can be evaluated by simulation if some previous data is available, and would provide more insight into the results that can be expected. Test plans can be of different types:

Traditional plans: These plans consist of equally spaced test stress levels and the specimens are equally divided amongst the stress levels.

Optimal plans: These plans are carefully optimized using statistical techniques in order to determine stress levels and specimen quantities. Depending on the underlying distribution (which can be obtained from previous data and expert opinion), different plans are available.

## CHAPTER 4

### DATA ACQUISITION SYSTEM

#### Introduction

This chapter describes the Data Acquisition system (DAQ) that was developed for use in this project. This chapter discusses the need for development of such a system in the following few paragraphs. The next section gives an overview of the system's functionality followed by detailed analysis of the design specifications considered. The prototype and the actual system are then described in the subsequent sections. Finally, features of the human machine interface used to control the system are discussed.

In the previous chapter, statistical models were discussed for accelerated life testing and degradation testing. It is obvious from the discussion that failure data and degradation parameters need to be closely monitored for accurate prediction of life, because doing so would minimize censorship, simplify the mathematics, and make the estimate as accurate as possible.

As discussed in the previous chapter, failure data of the electronic meters is required to predict the operational lifetime in the field and in order to obtain this failure data relatively quickly, the meters need to be operated at elevated stress conditions. Stresses that would induce failures in meters are temperature, voltage, vibration, and humidity, but because the existing testing apparatus does not have the capability of testing with stresses other than temperature, only temperature related failure modes are discussed in this thesis. Moreover, temperature is the most important stress factor and

almost every electronic component has a failure mode that is directly born out of temperature as stress. Future work will include other types of stresses and their effects.

By testing meters at elevated temperatures, errors and defects will be experienced at rates that exceed those occurring when a meter is operating in its design specified temperature range. Elevated temperatures are obtained in the lab by using environmental chambers which are scientific testing equipment that are used in the laboratory to simulate environments with required temperatures, humidity , pressure, dust, etc. They have access ports for instrumentation and wire connections, and are generally equipped with PLCs so that any profile of the stress (for example thermal shock, thermal ramp, etc.) can be programmed for simulation with a high degree of accuracy. Environmental chambers are expensive equipment and the chamber procured by EPRI for this project has the capability of simulating environments with a range of temperature from  $-35^{\circ}\text{C}$  to  $+75^{\circ}\text{C}$  and is hence limited in its functionality because of its temperature range.

The health of the meters can be determined by observing the LCD display because most new meters have a self-test algorithm in their DSP that will display an error on the LCD if there is a defect. This poses a complication since extreme conditions prevail in the interior of the chamber and it is inaccessible for observing the LCD displays on the meters during operation. The chamber can be shut off and allowed to cool down but that is a time consuming and labor intensive process. Moreover, LCDs themselves are sensitive components and they may cease to function even though the internal components function properly.

Alternately, the calibration infrared LED can be used to detect the health of the meter. Recall, from Chapter 2, that electronic meters have an infrared LED fitted in them, which is connected to an internal circuit to produce pulses at a rate proportional to the energy read by the meter. This LED is used for calibration purposes in the lab or field to determine the accuracy of the meter and commercially available test stations and hand held devices are available to measure the accuracy of meters by measuring the pulses originating from the LED. These devices may be used to continuously monitor the meters placed in the environmental chamber however, in doing so, such devices again are of less use because they are expensive, occupy large amounts of space and, most importantly, they will undergo the same aging that the meters experience, yielding errors and defects of their own. On the other hand, disconnecting the system, pulling the meters out and testing them outside is a time consuming process and will only provide interval censored data. This means that status of the meter can be monitored only after discrete periods of time. For example, if the inspection is done after every 1000 hours, a failure after just 300 hours will not be seen until the end of the 1000 hour interval. This will complicate the mathematical model and yield somewhat less accurate inferences of life expectancy.

Keeping the above limitations in mind, development of a Data Acquisition System was essential to monitor the health of the meters continuously and report if any meter fails or strays from specifications. The presence of a calibration infrared LED has been exploited in developing the DAQ. The LED is used for extracting continuous data from the inaccessible environmental chamber and hence facilitating the continuous monitoring of the health of the meters. The details of the system are discussed in this



chapter. The system also monitors temperature around the meter since the chamber's control system will monitor temperature at some other location in the chamber and there may be a gradient, especially if the chamber is large. Initially a prototype system was developed at Clemson University with a few meters. Once the system was fully functional, it was implemented at EPRI facility in the environmental chamber. This chapter first presents the overview of the functionality followed by analysis of the design specifications and the software considerations.

### Data Acquisition System

As mentioned above, the purpose of the DAQ is to gather two important data and deduce other information from them. The data that needs to be gathered are:

- 1) Energy accumulation
- 2) Temperature

A National Instruments<sup>®</sup> PXI system was supplied by EPRI for the project. PXI systems (PCI extensions for Instrumentation) are modular electronic instrumentation platforms whose technology was first introduced by National Instruments in late 1990's. These systems are based on standard computer buses and permit flexibility to build an instrumentation system as per the requirements. The system provided, consists of the several instrumentation devices, and are listed in Table 4.1.

Table 4.1 Instrumentation devices

Sr. No.	Device	Purpose
1	NI PXI 1042	Chassis to hold the controller and other acquisition devices
2	NI PXI 8106	On board controller with an Intel Pentium 4 processor, RAM and Hard Disk for programming environment.
3	NI PXI 4204	Analog input
4	NI PXI 4351	High resolution temperature / voltage acquisition card
5	NI PXI 6533	Digital I/O
6	SCB 68	Breakout board for connections
7	CB 68T	High resolution temperature / voltage breakout board with an onboard thermistor for Cold Junction Compensation

#### Energy and power calculation

As mentioned previously, apart from the LCD display, electronic meters generate pulses using an infrared LED which can be used to calculate energy accumulated. The LED's location is shown in Figure 4.1. Some other manufacturers may have this LED on the top of the meter. The watt-hours seen by the meter can be accurately calculated by developing the DAQ, and using it to count the infrared pulses.



Figure 4.1 Electronic watt-hour meter (source : GE I-210 manual)

The number of pulses is proportional to the energy accumulated and also depends on the Kh constant of the meter. For example if 15 watt-hours are seen, then a meter with Kh constant of 1 will emit 15 pulses where as a meter with Kh constant of 7.2 will emit only 2 pulses. This can be seen in Figure 4.2. By using the DAQ and comparing with a reference meter, whose accuracy is known, error, if any, can be calculated for the meters being tested.

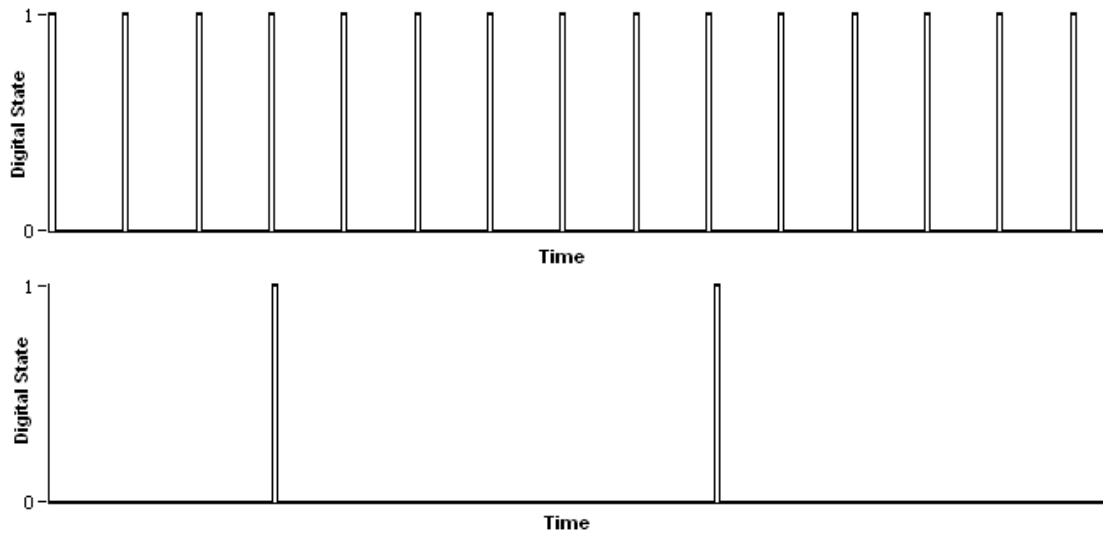


Figure 4.2 Infrared pulses emitted by meters with different Kh constants

The pulses emitted by the electronic meter are observed by using a phototransistor or a photodiode in a simple electronic circuit. A phototransistor is used rather than a photo diode since they have a higher responsivity to light. In order to capture the pulses emitted by the meter, an electronic circuit was designed. Figure 4.3 shows the designed circuit along with an ideal output.

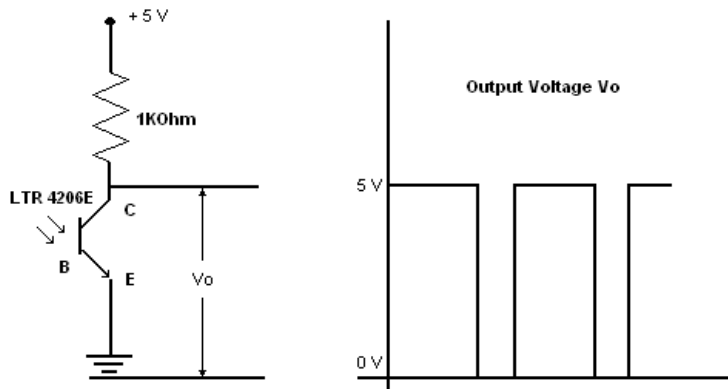


Figure 4.3 Pulse detection circuit

Whenever the photo LED on the meter emits a pulse, the base-emitter junction of the phototransistor (sensor) becomes saturated and the output drops close to 0 volts. In contrast, if the LED is off, the base-emitter junction will not be saturated and hence the output would be approximately 5 volts. An amplification circuit can be used to amplify the signals if attenuation is an issue. The 1 k $\Omega$  resistor is used in the circuit to limit the collector current since the maximum value of  $I_C$  for the phototransistors used is 10 mA.

The circuit is designed in such a way that each circuit draws only 5 mA and thus would lie within the limits of the component. This would sum up to 125 mA of current if 25 circuits are being used i.e. 25 meters are being tested simultaneously. Since the NI PXI 6533 device has a current source rated up to 800 mA, this current drawn will not overload the device.

This signal is then fed into a digital I/O board (in this case NI PXI 6533) which works based on standard TTL logic. All TTL logic circuits work with a 5 V supply, and a signal is considered as “high” if it is between 2.2V – 5V or “low” if it is between 0V – 0.8V. The voltage gap between 0.8V – 2.2V is considered a dead or indecisive band. Thus, an analog signal is converted to a digital signal comprising of only “high” and “low” (or 0s and 1s) and the problem of noise and other difficulties involved in analog signals are mitigated. Moreover is simpler to work with in software. The schematic of the connections is shown in Figure 4.4

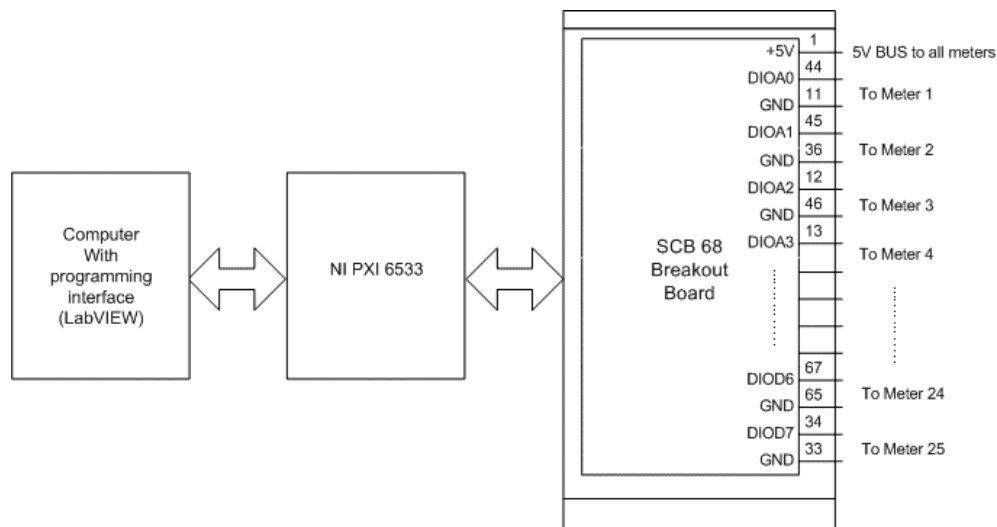
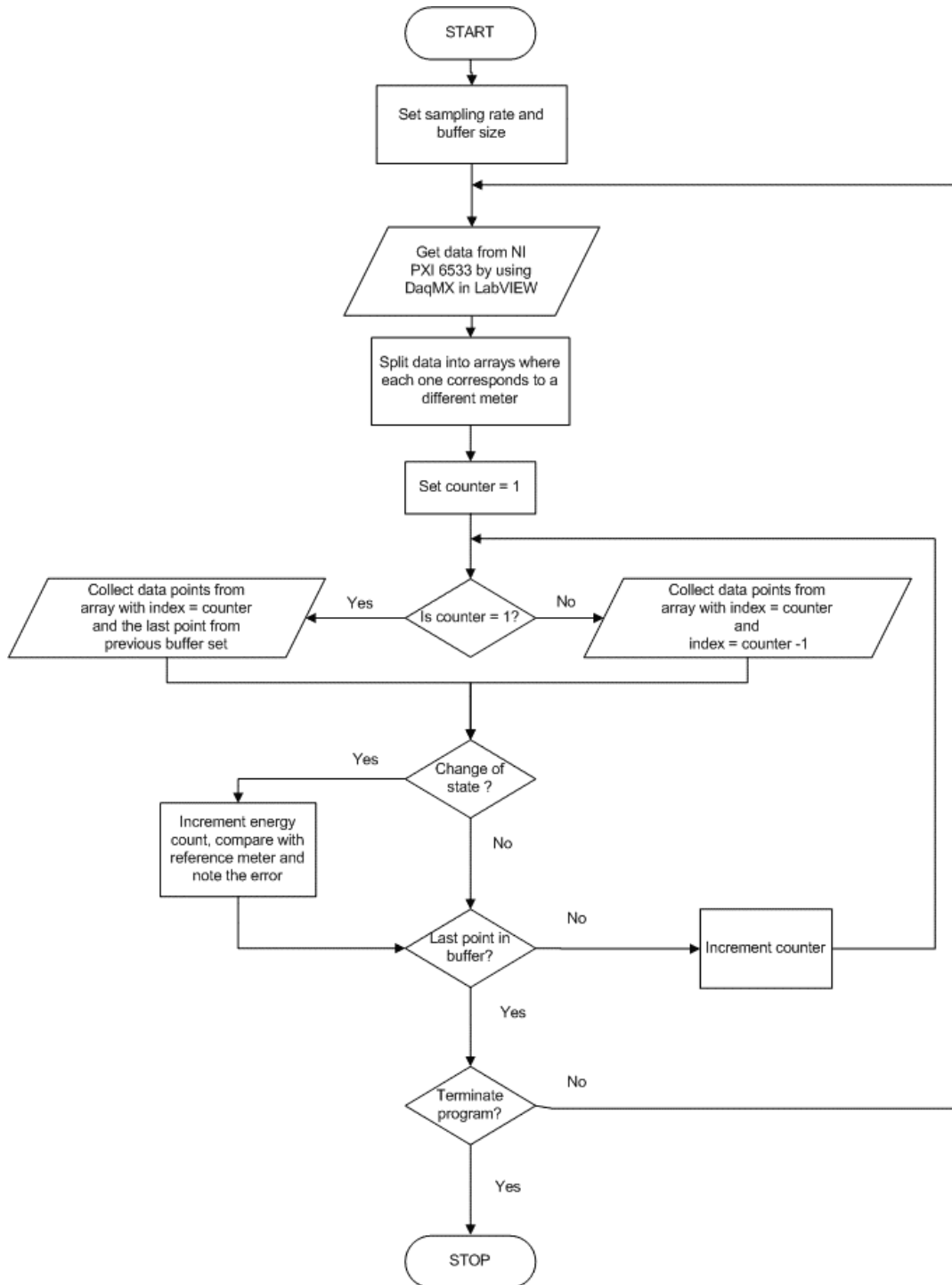


Figure 4.4 Schematic of the software / hardware interface

The device SCB 68, known as a breakout board, is basically a terminal block for National Instruments devices. The pins on the SCB 68 are digital I/O, analog I/O, power supply, trigger and ground (reference) connections. Depending on the DAQ device it is connected to, each pin corresponds to a different connection type. In our case, it is connected to NI PXI 6533 and the pin-out diagram for this configuration is given in the Appendix A. The NI PXI 6533 has four digital I/O ports (named A, B, C and D) with each port having eight lines (0 – 7), making it possible to monitor up to 32 inputs at a time. As depicted in the schematic above, the 5V supply is used as a common bus for all the sensors. The references are connected separately at each LED, but all tied together on the board thereby providing a common ground. The NI PXI 6533 is then connected with the computer and communication is established through software drivers. A programming language is required to control and communicate with the hardware. The LabVIEW graphical programming language is the recommended software by National

Instruments for their devices and is used in the project since it is also easier to work with than C or other middle level languages. LabVIEW is a dataflow programming language which means programs are written by placing blocks or figures in the workspace rather than writing lines of code. The program for this application has been provided in the Appendix C. The algorithm for the software is displayed in Figure 4.5 in the form of a flowchart.





#### Figure 4.5 Flowchart of the energy calculation algorithm

In developing the DAQ, the hardware design and software considerations that are important for the proper functionality of the system were taken into account. These considerations are further discussed as follows:

##### *Detector selection*

As per IEC 62052-11 and ANSI C.12 standards pertaining to electricity metering, the photo LEDs on the meters should emit pulses in the infrared band of wavelengths. The required range is from 550nm – 1000nm. Most commercially available infrared photo LEDs are in the band of 800nm – 900nm and therefore it was assumed that meter manufacturers use LEDs of the similar range in their products. This hypothesis was tested in the lab and proved to be accurate for the tested meters. A matching phototransistor is essential to detect the pulses. Otherwise the energy of other wavelengths of light will not be sufficient to forward bias the base-emitter junction of the phototransistor. This data is generally provided in datasheets of the detector manufacturer. In this project, photodetectors from Lite-ON<sup>®</sup> (part # LTR 4206E) and RadioShack<sup>®</sup> (part # 276-145) were used. The graph of sensitivity vs. wavelength of such detectors is shown in Figure 4.6.

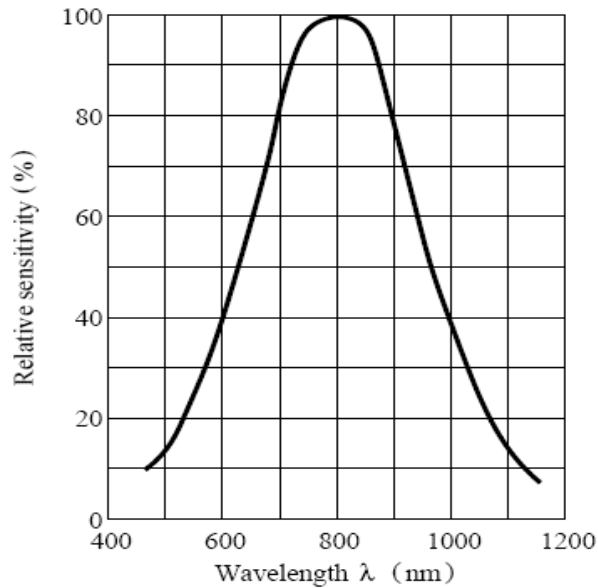


Figure 4.6 Relative sensitivity vs. Wavelength  
 (Source: Lite-ON (part # LTR 4206E) photo transistor data sheets)

### *Orientation*

Orienting the photo detector correctly with the photo LED is important. If it is not aligned properly, the IR rays will not fall on the substrate and the base-emitter junction will not become saturated resulting in a lower output voltage or even no voltage at all. Again, this data is generally provided by the manufacturer in the data specification sheets and is shown in Figure 4.7. Unlike wavelength which is more or less the same with most phototransistor manufacturers, the view angle varies greatly. There are models that start with 5° and extend up to 50° of viewing angle. The viewing angle of a phototransistor is the range angle, from the center, to which the phototransistor is sensitive. In other words, light rays from any angle within the specified viewing angle of the device can saturate the base-emitter junction and can make the device operate. The models selected were those

which had sensitivity over  $5^\circ$  on either side since a wider viewing angle may excite the system by some stray signals.

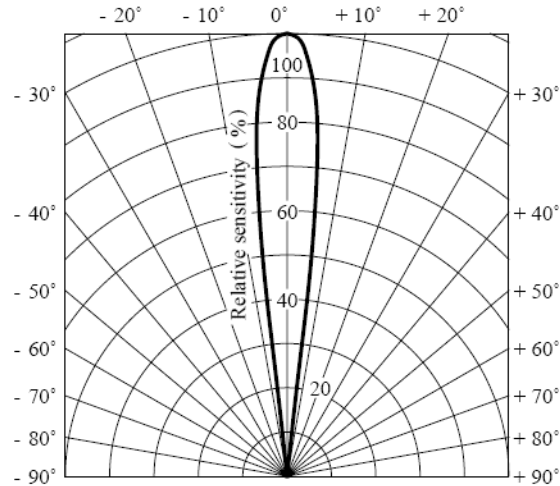


Figure 4.7 Relative sensitivity vs. viewing angle  
(Source: Lite-ON (part # LTR 4206E) photo transistor data sheets)

Different meters contain the calibration LEDs at different locations. Some may have them on top, while others have them in the front. The test set-up that is being used presently and EPRI has the sensors mounted onto the polycarbonate covers of the meters, by drilling holes into them. Such a setup was deemed unfit for the long-term testing, since every meter replaced would have to be fit with a new sensor. Flexible goosenecks were determined to be the best choice to make the DAQ system adjustable, so that it can be used for any brand of meters, for orienting the sensor directly onto the LED on that meter. Customized goosenecks were procured from Moffatt<sup>®</sup> products after considering the specifications such as length, diameter, flexibility and temperature coefficient of expansion and the sensor was fixed onto the gooseneck using LED holders that were specially machined at the Clemson University shop. The addition of the goosenecks to

the DAQ system has added flexibility to it, and can now accommodate meters of any brand and LED orientation as shown in Figure 4.8.

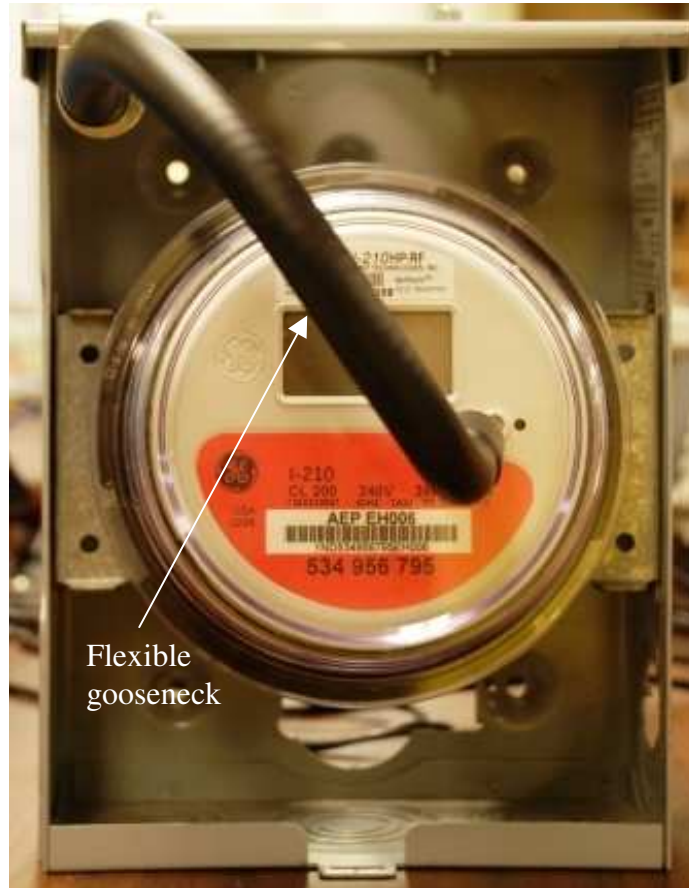


Figure 4.8 Illustration of flexible gooseneck

### *Temperature range*

Since the sensor is also inside the environmental chamber, the stress on the meter also affects the sensor. Therefore it is advisable to use military grade phototransistors that work over a wider range of temperatures. Commercial grade phototransistors are being used in the project at its present stage since the testing is being done only up to a temperature of 75°C. The commercial phototransistors have an operating range of -40°C

to 85°C. Alternately a fiber optic cable can be used to draw the rays outside the chamber and the phototransistor can be fixed outside, if operating ranges are expanded in future.

### *Sampling rate and buffer size*

In the software, two important quantities need to be entered appropriately to ensure proper sampling of the data. These quantities have been made user editable and hence adds to the flexibility of the DAQ to be deployed for other applications as well.

For a digital I/O board, a continuous signal is sampled into a number of discrete samples. The speed at which the sampling is done at is determined by the sampling rate, or sampling frequency. For example, if the sampling rate is 1 kHz, then a sample of the continuous signal is taken every 1 millisecond. These samples are digitized using an ADC and defined as “high” or “low” using TTL logic. The sampling frequency should be sufficiently high to ensure that no pulses are missed because the pulse width is quite small (in the order of 2-5 ms). The need for a sufficient sampling rate is illustrated in Figure 4.9 where several pulses are missed by the DAQ.

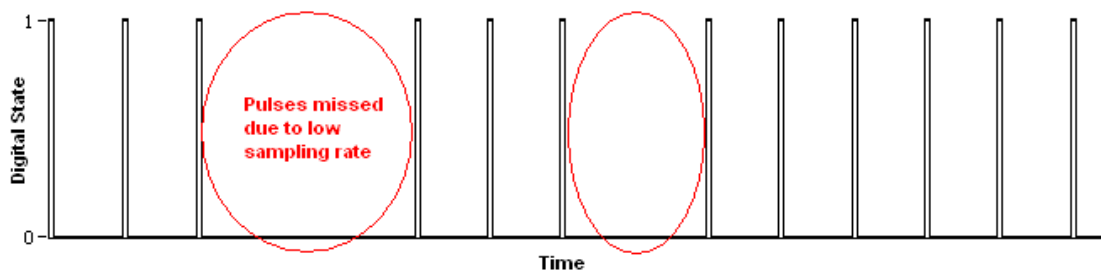


Figure 4.9 Effect of slow sampling rate

The other quantity which is important in the software is number of samples. The number of samples, and thus the buffer size, needs to be sufficiently large so that the signal is periodic. Although this is not important for energy calculation (since energy is just accumulation of the pulses), it is important for determining power since the time period between pulses is used to calculate power. It is necessary for the signal to be periodic to accomplish this and therefore the buffer size should be sufficiently large to capture at least two pulses.

#### Temperature measurement

Temperature can be measured using various kinds of instruments. Some of these are thermometers, Resistive Temperature Detectors (RTDs), thermistors, thermocouples, infrared devices, and pyrometers. While thermometers and infrared devices are just as accurate as the others, they are expensive and their output is not in the form of voltage and hence difficult to interface with the DAQ system. RTDs, thermocouples and thermistors can give an output in the form of voltage with relation to ambient temperature.

RTDs and thermistors are very accurate devices and can determine the temperature with very high accuracy, and they are primarily devices whose resistivity changes with temperature. Thus using a constant current source and measuring the voltage drop across them, the ambient temperature can be determined. However, they have certain disadvantages compared to thermocouples.

1. They are delicate devices and work only over a smaller range of temperature, and they are used for accurate temperature measurement rather than rugged use.
2. They require an additional current source to create an output voltage.

For the reasons mentioned above, thermocouples are used in the project because they are simple, inexpensive and rugged devices. Thermocouples work based on the Seebeck effect which states that when two dissimilar metals are fused to form a junction, a potential difference is developed and it is proportional to the temperature gradient between the two ends of the junction.

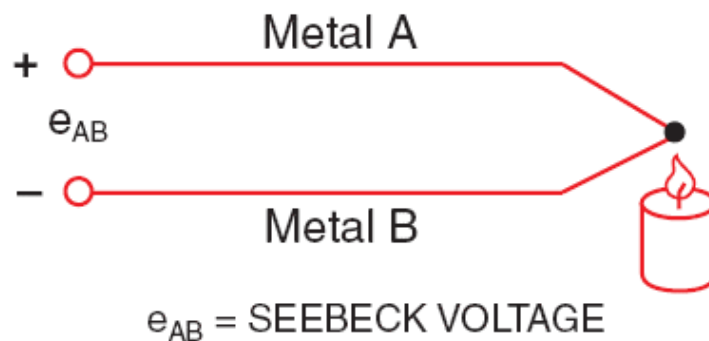


Figure 4.10 Thermocouple illustration  
(Source: [www.omega.com](http://www.omega.com))

Theoretically any two metals fused will exhibit thermionic or Seebeck effect. But because of certain desirable characteristics, a list of metal pairs has been standardized by IEC / ANSI. The pairs differ in the output voltage/ $^{\circ}\text{C}$ , ruggedness, temperature range and chemical properties. Table 4.2 shows commonly used types along with their nomenclature, temperature range, output voltage range and special characteristics.

Table 4.2 List of thermocouple types with characteristics

Type	Temperature range (°C)	Metals	Output voltage range (mV)	Special characteristics
<b>K</b>	-270 to 1370	chromel-alumel	-5.89 to 54.88	Nickel is magnetic and hence sees a step change at curie point 354 degrees
<b>J</b>	-210 to 1200	iron-constantan	-8.09 to 69.55	Old type and not used unless equipment cannot accept newer types
<b>N</b>	-270 to 1300	nicrosil-nisil	-3.99 to 47.51	Stable and oxidation resistant. Therefore used for high temperature applications
<b>R</b>	0 to 1760	platinum-rhodium	1.93 to 21.103	Low sensitivity and expensive but very stable and hence used only in high temperature measurements
<b>S</b>	0 to 1760	platinum-rhodium	1.87 to 18.693	Very stable and hence used only in high temperature measurements
<b>T</b>	-270 to 400	copper-constantan	-5.60 to 20.87	Both metals are not magnetic and hence used for applications in magnetic fields. High sensitivity
<b>E</b>	-270 to 1000	chromel-constantan	-8.8 to 76.37	High output sensitivity. Generally used for cryogenic applications
<b>B</b>	0 to 1820	platinum-rhodium	0.291 to 13.82	Low sensitivity and expensive but very stable and hence used only in high temperature measurements



Since it was desired to measure both positive and negative voltages, thermocouple type T was chosen to be used in this project. Type T also has a high sensitivity and hence results in more accurate results.

Thermocouples have a certain issues that need to be handled before temperature calculations can be made. These are discussed below in the following sub-sections.

### *Cold Junction compensation*

The point at which the thermocouple wire is connected to the terminals of the measuring device forms another junction and hence produces a voltage proportional the temperature of that junction. This junction has been traditionally called the Cold-Junction because thermocouples were traditionally used to measure high temperatures and this junction, by comparison, is colder than the location of the actual thermocouple junction. The cold-junction voltage can be compensated for either by using hardware compensation or a software algorithm. This process is called Cold Junction Compensation (CJC). In hardware compensation, an electronic circuit is constructed such that the circuit produces equal and opposite voltage to cancel the cold-junction voltage. Although this would be more accurate than the software compensation method, it is expensive because each thermocouple would require its own compensation circuit.

Alternately, the temperature of the cold-junction can be measured and the voltage can be canceled out using software algorithm. This method is presently easier to deal with since computer processor speeds have increased tremendously but in the past, it was a burden on the processor power resulting in delayed measurements.

## Noise

The output voltage of the thermocouples is in the order of millivolts and hence is susceptible to high frequency electromagnetic noise. This can be observed in the graph shown in Figure 4.11.

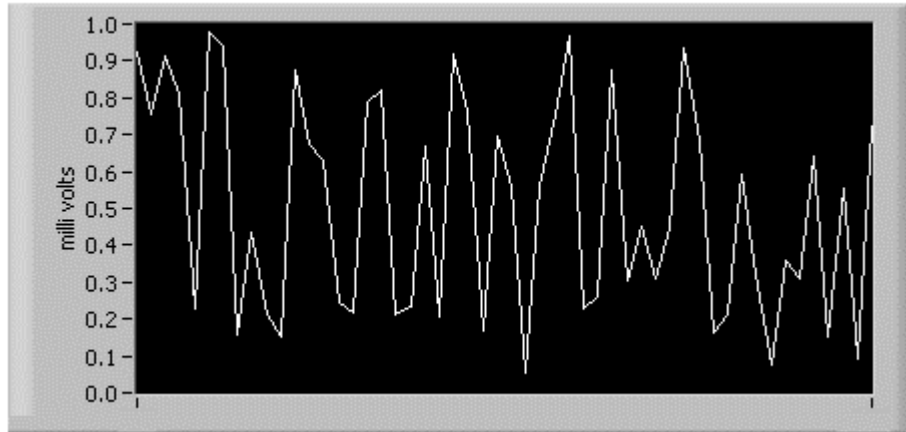


Figure 4.11 Thermocouple output contaminated with noise

Thermocouples are used in industrial environments and electromagnetic noise from tube lights and HID lights is sufficient to interfere with the voltage signal of the thermocouple and hence yield erroneous results. Therefore while selecting the thermocouples, the wires should be shielded, twisted pair and the length should be as small as possible. Additionally, a filter should be used which may be a physical RC filter, or the realization of the desired transfer function using software.

After the measurement issues are handled, the voltage, or emf, measured needs to be realized as temperature through a non-linear relationship. The relation can be obtained by measuring temperature and voltage at different points. The equation can then be

estimated by the use of curve fitting algorithms. Such coefficients have been observed over the years and are now standardized for different types of thermocouples by National Institute of Standards and Technology (NIST). The general form of the equation for determining the temperature is of the form shown below.

$$T = a_0 + a_1E + a_2E^2 + a_3E^3 + a_4E^4 + \dots + a_nE^n \quad (4.1)$$

Where  $a_0, a_1, a_2 \dots a_n$  are coefficients available on NIST website for different types of thermocouples ([www.nist.gov](http://www.nist.gov))

$E$  is the emf or voltage observed

#### Prototype

The development of the data acquisition system was done at Clemson University. In order to develop the data acquisition system, the meters were required to be in an operational state. This was required to gain insight into the pulsing circuit and determine the wavelength and the width of the IR rays emitted by the LED. Testing the accuracy of the software also required knowledge of the power seen by the meters and whether the meters are pulsing at a corresponding rate. A design of the flexible mounting system was also to be decided, and in order to do so, a prototype had to be set up to mimic the actual EPRI environmental chamber setup.

The PQIA lab is supplied by a 480V source and connected to a 500 kVA dedicated transformer. A 480/240 transformer is used to step down the voltage to 240 V phase-phase. This is used to feed a 6  $\Omega$  resistor bank that provides a load of 7200 W or 40A. Three meters are connected in series and the leads are kept as short as possible to

avoid voltage drop. The meter casings are strapped on to the resistor bank, to hold them in a fixed position, and safety purposes. Heavy gauge conductors, 6 AWG, are used to provide a path with negligible voltage drop, and these wires perform well since they have a small resistivity of  $2.12 \Omega / \text{mile}$ . This enables all the meters to see the same voltage and current and hence emit same number of pulses at the same rate. Phototransistor sensors are held in position using the flexible gooseneck apparatus purchased, as discussed earlier. Thermocouples are used for temperature sensing. Cold Junction Compensation and noise filtering are handled by software. The NI CB 68T breakout board has an onboard thermistor to measure the temperature of the cold junction and is used in simulating an artificial voltage of opposite polarity in the software algorithm for CJC. The schematic and the actual configuration are shown in Figure 4.12.

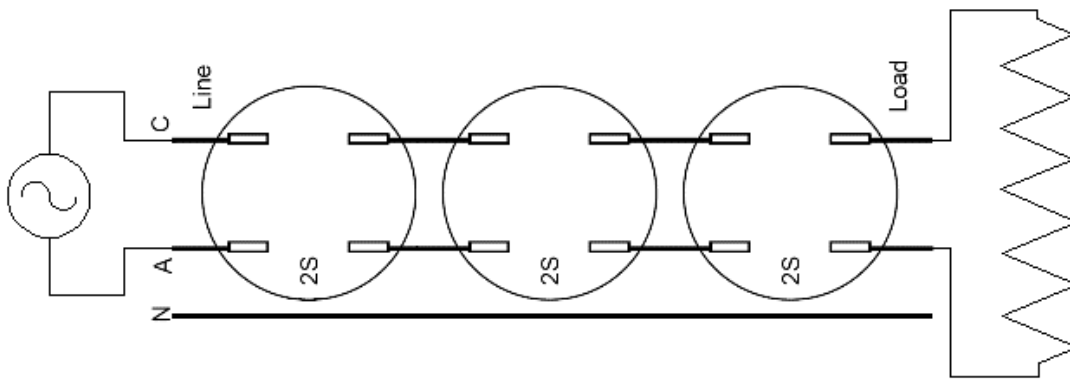


Figure 4.12 Schematic of the test set-up

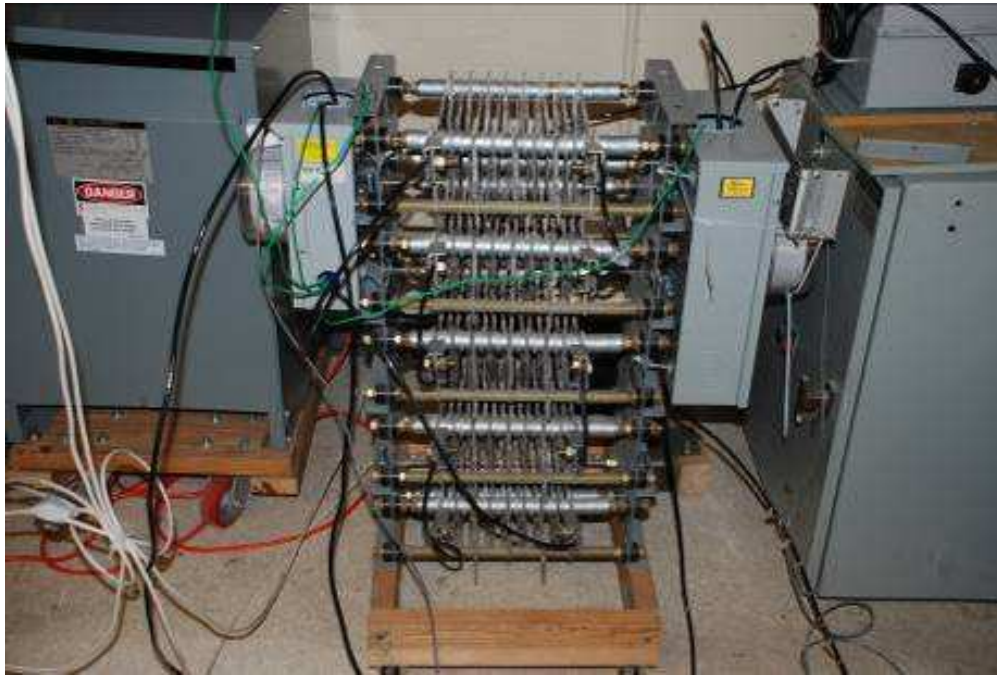


Figure 4.13 Experimental set-up showing the resistor bank, meters and transformer



Figure 4.14 The entire prototype

### Actual system at EPRI

For the purpose of this research project, an Envirotronics™ environmental chamber was procured by EPRI for environmental testing of the electronic meters. The chamber is designed to provide both temperature control, and humidity control when retrofit with additional components. At present the chamber does not possess humidity control apparatus, with the exception of a pump, to dry the environment inside, in order to avoid ice build-up during low temperature operation. The chamber is capable of heating up to +80°C and cooling down to -35°C, and uses a PLC (model: Mitsubishi FX-48MR) for the control. The controller can be programmed to generate any temperature profile as required, for example, it can do a ramp increase, thermal cycling, etc. When cycling temperature, the chamber requires approximately 12 hours to change from minimum temperature to the maximum temperature and vice-versa. This limitation is attributed to the large volume of the chamber that needs to be cooled or heated. Due to this limitation, stress profiles like thermal shock (sudden change from high to low temperatures or vice-versa) cannot be realized. A photo of the chamber at the EPRI facility is provided in Figure 4.15.



Figure 4.15 Envirotronics Chamber at EPRI facility

The meter test set-up at EPRI was developed inside the environmental chamber. The goal was to test electronic watt-hour meters, under extreme environmental conditions, and under load, as they would operate in the field. All the meters that were tested, were residential CL200 (Class 200) meters, that are rated for a load current of 200 amperes.

In order to test the meters for accuracy, it is not necessary to load the meter to its full capacity. Manufacturers provide a Test Amperes (TA) rating, at which the accuracy of the meter would mimic the accuracy at full load of 200 amps, and the TA rating for the meters being tested was 30A. The meters were connected in series as shown in the schematic in Figure 4.16, and hence would all see the same load current. The reference meter was placed outside the chamber so that it does not experience the stresses caused by extreme environmental conditions. The leads were made of heavy gauge wires and were kept as short as possible to avoid voltage drop between the meters.

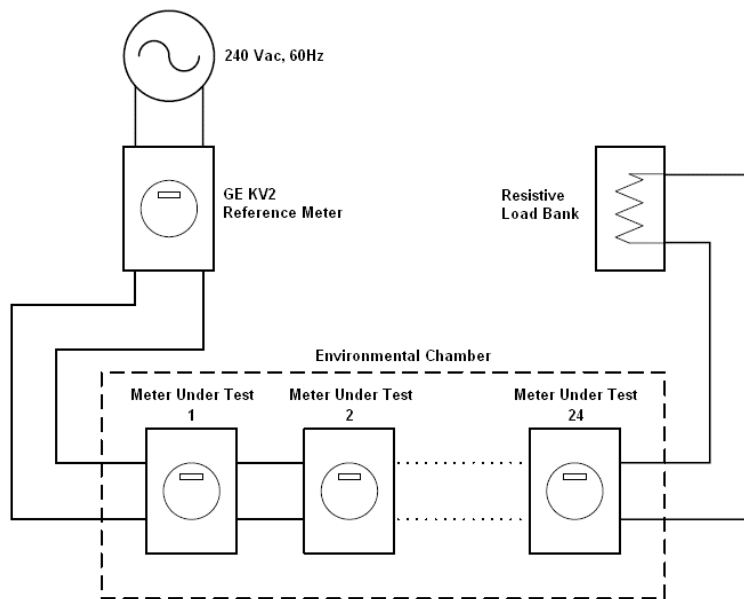


Figure 4.16 Schematic of the experiment

The load bank used was made up of resistive elements so that the power factor can be maintained at unity. The system can test 24 meters at one time, and the physical layout of the meters is shown in Figure 4.17. Twelve meters were fixed on one side of the wooden plank and the remaining on the other side, and this topology was preferred to



using another plank for fixing the other twelve meters, because the distance between the meters was desired to be minimum to reduce thermal gradient.



Figure 4.17 The actual test set-up at EPRI

The temperature of the chamber is measured by the chamber's control system. However, the control system uses only a few temperature sensing devices confined to just one part of the entire chamber, and hence would not represent the temperature around the meters, especially since the chamber has a large volume. Thermal gradient of up to four degrees has been observed. In order to accurately measure the temperature around the meters, nine thermocouples were placed at different locations on both sides of the wooden plank and temperature was calculated independently for each of them using software as described in previous sections. The thermocouples used were of type T and were shielded to minimize disturbance from electromagnetic noise signals.

The energy readings of the meters were sensed using optical sensors (phototransistors) as described in the previous sections. Phototransistors were selected to match with the wavelength of the pulses emitted by the infrared LED and, to match with the temperature range of operations inside the chamber. Care was taken to align the phototransistor with the infrared LEDs on the meters and for achieving the alignment, the phototransistors were directly mounted onto the polycarbonate cover of the meters. The flexible goosenecks used in the prototype have not been implemented in the chamber yet, and will be done in the future. All the wiring was brought out of the chamber through the 4 inch wide ducts on the walls of the chamber, and the ducts were plugged with foam so that there is no leakage of temperature.

One of the drawbacks of this chamber is the fact that it is limited in its range of operations. The meters are designed to operate with in  $-35^{\circ}\text{C}$  to  $+80^{\circ}\text{C}$ , and the maximum limits of the environmental chamber are not sufficiently large enough to cause acceleration of failure or defects. Another limitation of the chamber is the speed at which it can ramp up or down the temperature. Since the chamber is quite large, it cannot provide a fast rate of change of temperature which is required to perform accelerated life testing with thermal cycling.

### Human Machine Interface

In the previous sections, hardware specifications for data acquisition were discussed, followed by, a description of the prototype in the PQIA lab and the actual system at EPRI facility. As mentioned earlier, communication with hardware, data

logging, and analysis algorithms require a software program to perform real-time calculations. Recall from Table 4.1, that the procured PXI system contains NI PXI 8106, which is an onboard computer that runs on Windows operating system. LabVIEW 8.0 has been installed on this system for the purpose of writing programs, and enables it to interface with the other NI instrumentation devices that are used. LabVIEW is a dataflow programming language whose programs are called Virtual Instruments (VIs), which are essentially interfaces between users and instruments, and therefore also called Human Machine Interfaces (HMI). They are very different from conventional programming languages which are based on written lines of code.

When LabVIEW programming environment is started, the user is presented with two windows: front panel and block diagram. On the front panel, a user can place controls and indicators for data input and output operations. Controls, or input methods, can be of different types such as knobs, dials, sliders, text boxes, buttons, etc. Indicators, or output methods, comprise of progress bars, LED indicators, text boxes, graphs, etc. When controls or indicators are placed on the front panel, the block diagram will automatically be populated with the items that were placed on the front panel. Hardware interface blocks and other programming functions are present as icons, which can be placed on the block diagram, and using wires, the components can be connected such that the data flow occurs as: Input → Programming logic → Output. This is depicted in the Figure 4.18

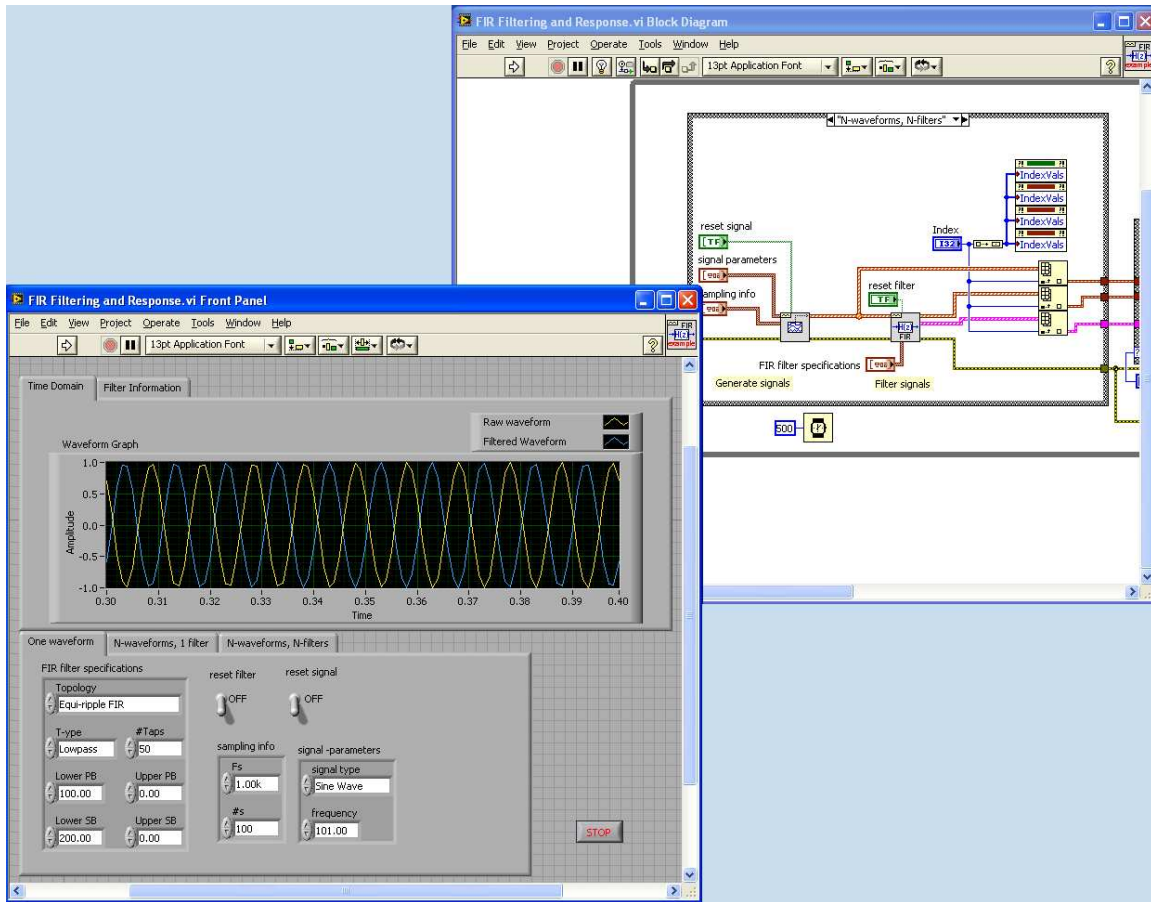


Figure 4.18 Illustration of front panel and block diagram in LabVIEW

A VI was developed in LabVIEW for the meter testing project, and while doing so, care was taken to make it as simple, user-friendly, and informative as possible. The code (block diagram) for the software is given in Appendix C. In making the VI, additional code was written, which is not a routine feature in LabVIEW, to represent all the information on the computer screen without having to scroll or switch tabs.

On the initial execution of the HMI, a dialog box appears in which the manufacturer details can be entered as shown in Figure 4.19.

	Manufacturer	Model	Kh Constant
1	Itron	unknown	1
2	Itron	unknown	1
3	Itron	unknown	1
4	Itron	unknown	1
5	Itron	unknown	1
6	unknown	unknown	1
7	unknown	unknown	1
8	unknown	unknown	1
9	Landis & Gyr	Focus	7.2
10	Landis & Gyr	Focus	7.2
11	Landis & Gyr	Focus	7.2
12	Landis & Gyr	Focus	7.2
13	Landis & Gyr	Focus	7.2
14	unknown	unknown	1
15	unknown	unknown	1
16	unknown	unknown	1
17	Landis & Gyr	Focus	7.2
18	unknown	unknown	1
19	unknown	unknown	1
20	unknown	unknown	1
21	unknown	unknown	1
22	unknown	unknown	1
23	unknown	unknown	1
24	unknown	unknown	1

Figure 4.19 Dialog box for manufacturer’s details

The manufacturer’s details include the brand, model, and the Kh constant. If the brand and model are left unattended, the default values of “unknown” will be populated. The Kh constants are important, since they are multiplication factors for the energy readings of the meters; the default value of 1 will be taken, if the field is left blank.

For example, if the Kh value for a meter with a Kh constant of 7.2 is left blank, the software will calculate energy read as 2 watt-hours for actual consumed energy of 15 watt-hours, because each pulse would then represent one watt-hour, since the default

value is one. This dialog box can also be accessed during execution from 'settings' as explained later.

After entering the data into the dialog box and clicking the 'OK' button, the program operation begins. The HMI contains four panes shown in Figure 4.20. The panes are reference data, environmental chamber layout, user inputs, and the variable pane. The first three panes remain constant for all pages and only the variable pane changes for each of the pages, namely: *main*, *meter* and *temperature*. The default variable page is the *main* or *summary* page, which gives a synopsis of the state of all the meters. Each meter box has an energy output display, a power output display and an LED indicator. The energy is calculated by accumulating pulses from the beginning of program execution and multiplying the result by the Kh constant of the corresponding meter as entered into the dialog box earlier. The power is calculated real-time by calculating the time period between pulses. The LED indicator glows if that particular meter catastrophically fails or drifts in accuracy beyond specifications. During the program execution, clicking on summary button, in the reference data pane, changes the variable pane back to the *main* page. Clicking on any meter box changes the variable page to the corresponding *meter* page while the remaining three pages stay fixed.



Figure 4.20 Main page of the DAQ software

The components in each pane, except variable pane, are briefly explained as follows. The variable pane changes according to the page viewed.

The reference data pane contains the following components, as seen in Figure 4.20:

- Reference meter pulses (waveform)
- Reference meter energy and power
- Elapsed time
- Settings, temperature, and summary tabs (menu)

The reference data pane is fixed and never hidden during any time of the execution to ensure that the settings and reference meter data are always visible and accessible. The waveform shows the pulses emitted by the reference calibrated meter, which is placed outside the environmental chamber.

The reference meter energy field displays the cumulative energy seen by this meter, in watt-hours, since the initial execution of the program. The energy seen is determined by counting the number of pulses emitted and multiplying by the Kh constant. Since the reference meter is not replaced during testing, its Kh constant is not capable of being altered and is hardcoded into the program.

The reference meter power field displays the real-time power as seen by the reference meter and is calculated by calculating the time period between the pulses. This is then converted into power by the Equation 4.1:

$$Power = \frac{3600 \times Kh \text{ const}}{\text{time period between pulses}} \quad (4.1)$$

The elapsed time field shows the time, in seconds, since the initial execution of the program. The menu comprises of settings, temperature and summary buttons. Clicking on ‘Settings’ leads to a page where the user can access the meter manufacturer data dialog box, adjust email settings, adjust data file storage location, or reset all the meter readings to zero. The ‘temperature’ button leads to the temperature page which is discussed in detail later. The ‘summary’ button brings the program back to the *main* page from anywhere in the program.



The environmental chamber layout pane also stays fixed and is never hidden during the program execution. This pane illustrates physical layout of the meters in the environmental chamber as shown in the previous section in Figure 4.17. Each meter is represented by a LED indicator and turns red if the meter fails or drifts in accuracy. The advantage of laying out the LED indicators in the same manner as the physical layout in the chamber is that, in the event of a failure, the user can directly pinpoint the location inside the environmental chamber because the corresponding LED indicator will turn red. Necessary action can then be taken promptly without referring to the database of meters to find the location in the chamber.

Clicking on any LED indicator will take the user directly to the meter page and hence facilitates moving around the HMI easily. This feature is not a standard component of LabVIEW and additional code has been written to make the HMI more user-friendly.

The user input pane contains user inputs that make the HMI flexible and applicable to meters of any brand. This pane consists of four user inputs as described below:

- Error percentage
- Error duration
- Sampling rate
- Number of samples (buffer size)

The data acquisition system is built to not only to identify catastrophic failures, but to also determine the accuracy drift of the electronic meters with time at elevated temperatures. The HMI system continuously calculates energy accumulated by each

meter compares it with the reference meter, which is calibrated and placed outside the chamber. The ‘error percentage’ input specifies the limits of error, which the system needs to consider acceptable. For example, if error percentage is specified as 2%, then any error within  $\pm 2\%$  is considered acceptable and just recorded in the log file, while error greater than  $\pm 2\%$  would be considered as a catastrophic failure and the LEDs would turn on. The reason for adding this input is to add flexibility to the system, since different standards specify different limits of accuracy drift.

Short-term drift in accuracy for electronic meters is not uncommon, and sometimes, meters may drift outside specified band and return immediately. This condition cannot be considered a failure, and needs to be distinguished from actual accuracy related failures. The ‘error duration’ input specifies a period for which the observed error needs to be sustained in order to be considered a failure. For example, if the error margin is specified as 2% and error duration as 1 hour (= 3600 seconds), then an error beyond 2% sustained for one hour is considered a failure, where as, if the error returns into the 2% margin before the time period specified, it would not be considered an error.

The sampling rate and buffer size have been discussed in software considerations in the previous section of this chapter. To reiterate, sampling size should be selected such that no samples are missed by the DAQ (refer Figure 4.8). The buffer size (# of samples) needs to be sufficiently large so that at least two pulses are captured in order to make the waveform periodic. These settings can be adjusted real-time in the HMI which enables checking the graphs and adjusting the sampling information accordingly.

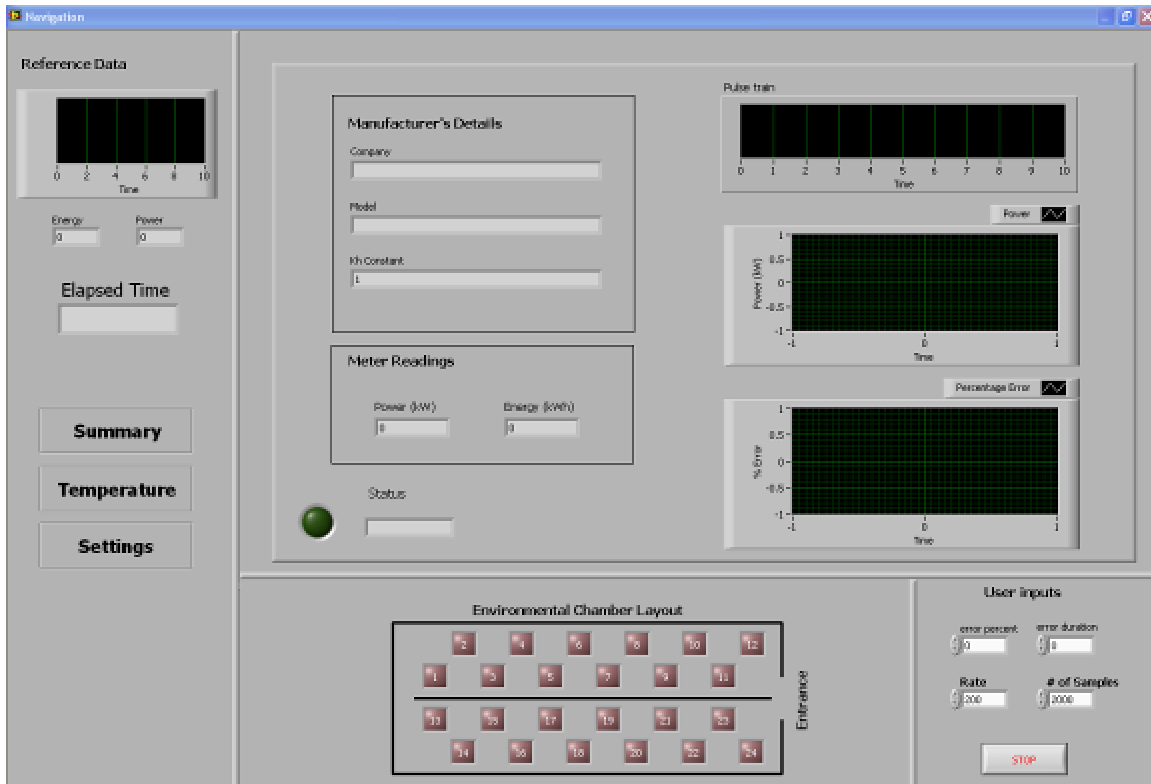


Figure 4.21 Meter page of the DAQ software

Clicking on any meter in the *main* page, or any of the LEDs in the environmental chamber pane changes the variable pane to the *meter page* of that corresponding meter as shown in Figure 4.21. The meter page shows more details of the meter when compared to the corresponding meter box on the *main* page. The items on the *meter page* are:

- Pulse output (waveform)
- Power and Energy fields
- Power output (waveform)
- Error percentage (waveform)
- Manufacturer's details

The pulses emitted are shown in the pulse output waveform whose scales are on autoset enabling them to adjust automatically as time changes. The power and energy fields display the same values as in the *main* page box of the corresponding meter. The power output waveform displays the last ten calculated outputs, and hence, the power fluctuations can be observed from this plot. Error percentage waveform displays the last ten error values, calculated by comparing with the reference meter. Manufacturer details are automatically populated from the initial dialog box and displayed on this page. The status LED performs the same function as the other LEDs described earlier, i.e. turn on when a meter fails or drifts in accuracy beyond specified limits.

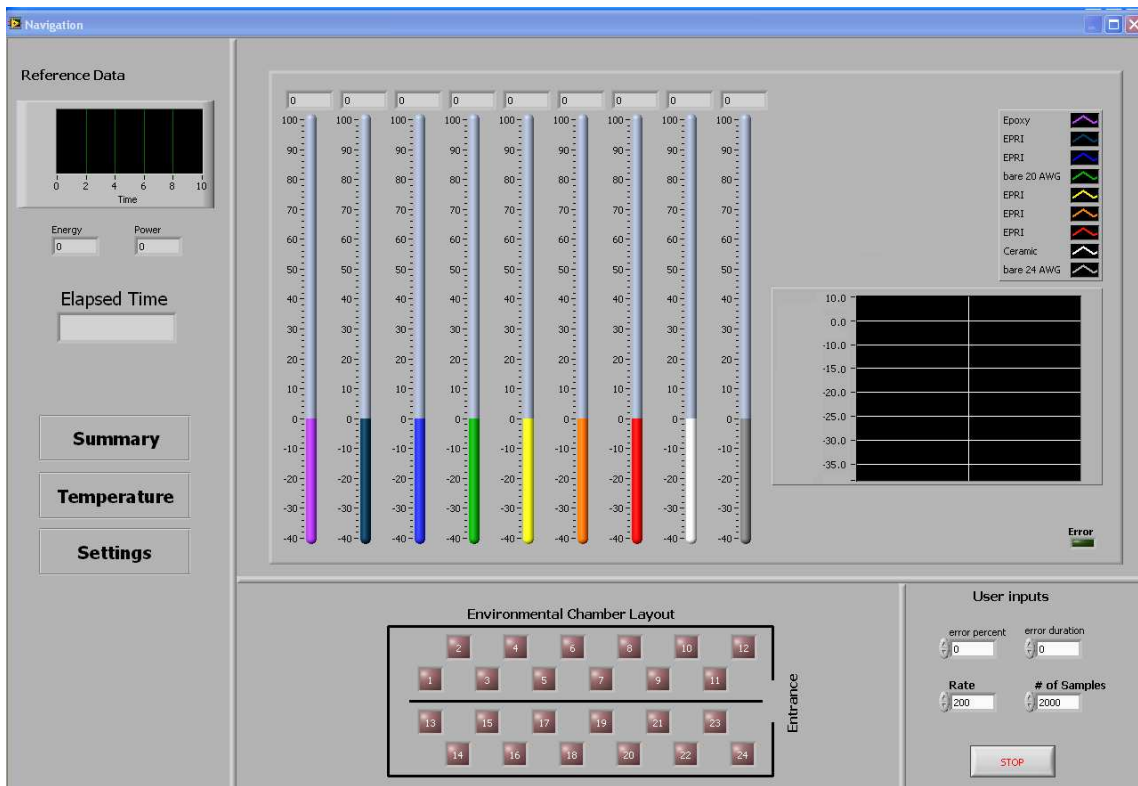


Figure 4.22 The temperature page of the DAQ software

The *temperature* page, as shown in Figure 4.22, can be reached by clicking on the temperature button in the reference data pane, from where the user can monitor the temperature of the chamber at different locations where the thermocouples have been placed. A total of nine thermocouples can be installed and monitored using this page. An average value of temperature can be used for the statistical calculations. The thermometers display the instantaneous temperature. The graph shows the last ten temperature points and automatically refreshes itself when new data is available.

Apart from the visible functions of the program on the HMI, a considerable amount of code was written to facilitate the storage of data. The program continuously monitors the health of the meters and generates daily and hourly reports in the form of text files. The data includes the meter ID, average temperature, power, energy, percentage error and status (health).

## CHAPTER 5

### TEST PLAN, RESULTS AND DISCUSSION

#### Test procedure

The initial test plan comprised of subjecting the electronic meters to elevated temperatures to yield thermal related failures that could be mapped to normal usage conditions using the Arrhenius equation. The engineers at EPRI determined the values of the elevated temperatures to be such that they remained within the IEC specifications, of -35 °C to 80 °C, for electricity metering [22, 23, 24, and 25]. However, the IEC specifications do not require the meters to be in an operational state, and they only specify that the meters to be exposed to the temperatures for a short duration of time. The test plan developed in conjunction with EPRI consisted of three sets of tests: high temperature tests, low temperature tests and thermal cycling tests. The details of the tests are:

High temperature test: The high temperature test comprises of testing twenty meters (of different brands and hence different topologies) in an environmental chamber with a constant stress level of 80 °C under load of 30 amperes at 240 V or 9600 W. The period of the test is 6 months. The objective of this test is to determine the effect of temperature on discrete electronic components such as capacitors and other semiconductor devices. One of the failure modes that is intended to be excited is the evaporation of electrolyte

from electrolytic capacitors present in power supplies and the signal conditioning part of the electronic meter, and would be indicated by a drift in accuracy of the meter.

Low temperature test: The low temperature test set comprises of testing twenty meters (again of different brands) in the environmental chamber with a constant stress level of  $-35^{\circ}\text{C}$  for a period of six months while under a load of 9600W. The objective of this test is again to analyze a failure which is defined as a catastrophic failure or drift in meter accuracy. Some of the failure modes are the deformation of plastic components, failure of LCD displays, and cracking of ribbon cables present inside the meter. Electrolyte present in capacitors also changes in viscosity, and hence changes its capacitance value, possibly affecting the accuracy of the electronic meter.

Thermal cycling: The thermal cycling test applies stress on the meter and its components, such as the solder joints on the printed circuit board, connectors, etc. Thermal cycle can be obtained in environmental chambers by programming the PLC that operates the chambers controls. The plan is to test twenty meters under load by cycling the temperature between  $-35^{\circ}\text{C}$  and  $80^{\circ}\text{C}$  for a period of four months. Due to the limitations of the environmental chamber at EPRI primarily due its large volume , thermal cycling takes approximately 10 hours to change from  $-35^{\circ}\text{C}$  to  $80^{\circ}\text{C}$  and vice-versa. The dwell time at the extreme temperatures is set to 2 hours making one complete cycle in a 24 hour period.

### Test results and discussion

As of the submission time of this thesis, the high temperature and low temperature tests have been completed, and the meters showed no failures. A failure of a meter was defined as either a catastrophic failure or a drift in accuracy greater than  $\pm 2\%$  as specified by IEC and ANSI standards. These tests were conducted before the completion of the development of the data acquisition system described in this thesis, and hence the meters were inspected at monthly intervals by shutting down the chamber and testing the meters using a UTEC 5800 calibration station. The results of the high temperature tests are shown in Figure 5.1

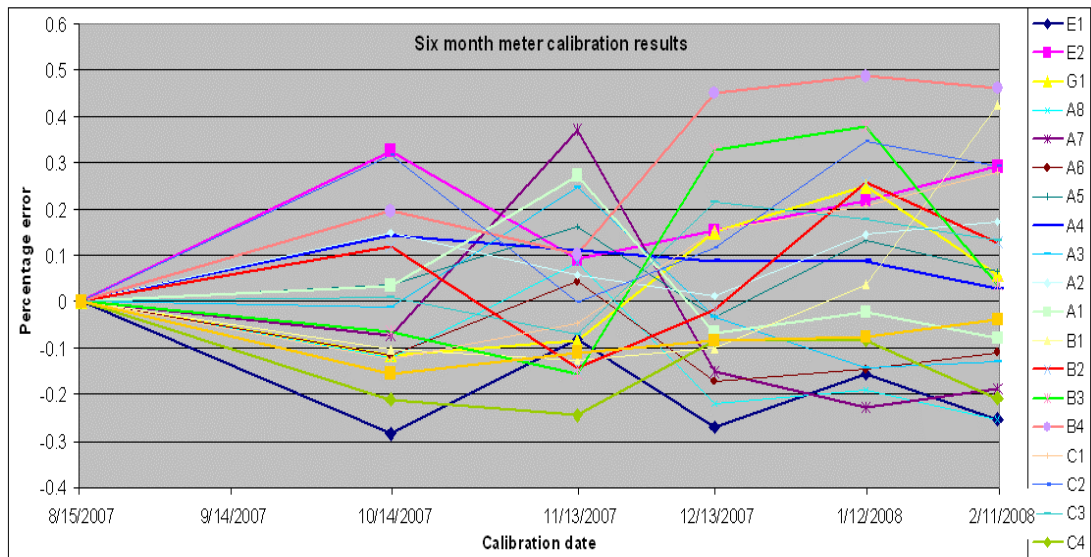


Figure 5.1 Calibration results for high temperature tests

From Figure 5.1 it can be seen that the drift in accuracy, in the 20 meters tested, did not show any pattern or trend, and is random. It can be observed from the figure that the maximum drift attained was approximately 0.5%, which is well with-in the IEC and



ANSI standards of 2%. Therefore the life prediction analysis that was discussed in Chapter 3 could not be used and no conclusions can be drawn regarding the predicted life of the electronic meters.

Thermal cycling tests will commence in September 2008 and the results will be available for analysis in December 2008, beyond the submission date of this thesis. Since no failure data from thermal tests are available as of today, no analysis can be performed.

From the analysis of the results the following conclusions regarding the high temperature and low temperature tests can be drawn:

- The present test results only confirm that the electronic meters that were tested conform to the ANSI and IEC standards of  $-35^{\circ}\text{C}$  to  $80^{\circ}\text{C}$ . They do not provide any failure data or insight into the failure mechanism.
- The meters were designed for a temperature range of  $-35^{\circ}\text{C}$  to  $85^{\circ}\text{C}$  and hence testing within the range of  $-35^{\circ}\text{C}$  to  $80^{\circ}\text{C}$  may not yield results because there is negligible acceleration in the failure mode
- In order to obtain failure data, two options are available: testing at higher levels of thermal stress, or testing for a longer duration of time.
- In order to obtain useful information regarding the life of the meters, failures from identical electronic meters is required, and the test plan comprising of testing small samples of different brands will not yield any useful information.

### Recommended test plan

In order to carry out the life prediction analysis, obtaining failure data is essential. The following recommended strategies may improve the probability of obtaining data in a timely fashion:

1. Conduct a pilot test with a few samples to gain insight into the failure mechanism. Such pilot test can provide useful information in deciding the number of samples to tests and appropriate stress levels. For example, a pilot test conducted on a few samples showed that a stress level of 125 °C induced failures in the control transformer for a particular brand of meters.
2. A decision needs to be made for the number of samples to be tested. The failure distribution parameters can be more closely predicted when a large number of failure times are available. Since we cannot expect all the meters to fail, a large number of samples must be tested. The samples decided to be tested should be of the same brand so that the failure mode occurs in all of them. For example, if 20 times-to-failure are required, at least 40 meters should be tested.
3. Two temperature levels need to be decided based on the pilot tests. The pilot test conducted at 125 °C showed that it would be sufficient to induced failures. 125 °C was chosen because it is 150% of the design stress level and is neither too less nor falls into the destruct levels. Hence 125 °C can be chosen as one elevated level. In order to map the relationship to the usage level another mid-level temperature is required and chosen as 100 °C. The DAQ can be used to continuously monitor the meters while testing at these temperatures.

4. More samples should be tested at lower temperature (100°C) so that more failures may be observed. The probability of failure is greater at high temperatures, and hence testing a few samples at higher temperatures is advisable. The decision on distribution of the samples relies on previous distribution data. For example, if 100 meters were available for testing, and 20 meters are required to fail at each stress level, then 30 meters should be placed at 125°C and 70 meters at 100°C.
5. For thermal cycling test, a steeper ramp rate is required to induce thermal stress on solder joints. This is a limitation of the environmental chamber and hence a new smaller chamber may need to be procured.

## CHAPTER 6

### ANALYSIS USING EXAMPLES

#### Introduction

Lab testing of electronic revenue meters began in August 2007 and two sets of tests have been conducted as of the submission of this thesis. The first test was conducted at a constant temperature of 80 °C, before the development of the DAQ described in Chapter 4, and the meter inspections were done manually at the end of each month for a period of six months. At the end of the six month period, none of the meters had failed, and the drift in accuracy was negligible and random. The second test was conducted at -35°C, also for a period of six months, and did not yield any failures. The reason for lack of failures or significant deviation in accuracy was determined to be the fact that the meters were designed for the test temperature range being used, and to observe any failures, either the stress or the testing time had to be increased significantly.

Since there is no data, life prediction analysis could not be performed on the meters. The reason for the lack of data was found to be the levels of stress used, and resulted in negligible acceleration of the failure mode. These stress levels were decided by EPRI engineers prior to this thesis. For the purpose of demonstration of the analysis procedure, two examples are provided in this chapter, which will illustrate the concepts explained in Chapter 3. The first problem deals with failure data analysis, while the second one analyzes degradation data.

### Failure data analysis

In the following problem, the data is obtained from accelerated testing experiments conducted on distribution system cable insulation, and the objective is to determine the life of electric cable insulation under design conditions. This data is taken from the datasets provided by Minitab software. When test results for the accelerated life tests of electronic meters are available, similar analysis will yield estimates of operational lifetime of the meters in the field.

Forty cable insulation specimens were subjected to elevated temperatures (twenty at 130 °C and the other twenty at 110 °C). These temperatures are approximately 50% greater than design stress (80 °C), which is acceptable, and do not lie within destruct levels, where definite failures would occur and yield no useful information. The data comes from a traditional test plan, because of the equal distribution of specimens between the two stress levels. In an optimal plan, specimens would be distributed as per some calculated statistic, which usually involves analysis of previously acquired life-data of the same component, and expert opinion. The insulation on the specimens is continuously monitored and times-to failure data is shown in Table 6.1.

Table 6.1 Failure data of insulation specimens

Temperature (°C)	Failure Time (Hours)	Censor	Design (°C)
130	2214	F	80
130	3128	F	
130	3147	F	
130	3308	F	
130	3545	F	
130	3620	C	
130	3987	F	
130	4348	F	
130	4373	F	
130	4735	C	
130	4925	F	
130	5117	F	
130	5351	F	
130	5355	F	
130	6226	F	
130	6947	F	
130	7304	F	
130	7919	F	
130	8290	F	
130	10183	F	

Temperature (°C)	Failure Time (Hours)	Censor	Design (°C)
110	7336	C	80
110	8702	F	
110	11143	C	
110	11769	F	
110	12090	F	
110	13218	F	
110	13513	F	
110	13673	F	
110	14482	F	
110	16289	F	
110	17610	F	
110	17784	F	
110	17822	F	
110	18397	F	
110	18806	F	
110	20975	F	
110	21900	C	
110	21900	C	
110	21900	C	
110	21900	C	

The test is stopped after 21900 hours, possibly because of a managerial decision, and thus resulting in data being right censored. Apart from the censored data after 21900 hours, there are some randomly censored data, for unknown reasons, that are identified by the letter C in the Censor column in the Table 6.1.

Once the data is accumulated, the analysis method follows the steps explained in Chapter 3 and can be depicted by the flowchart as follows:

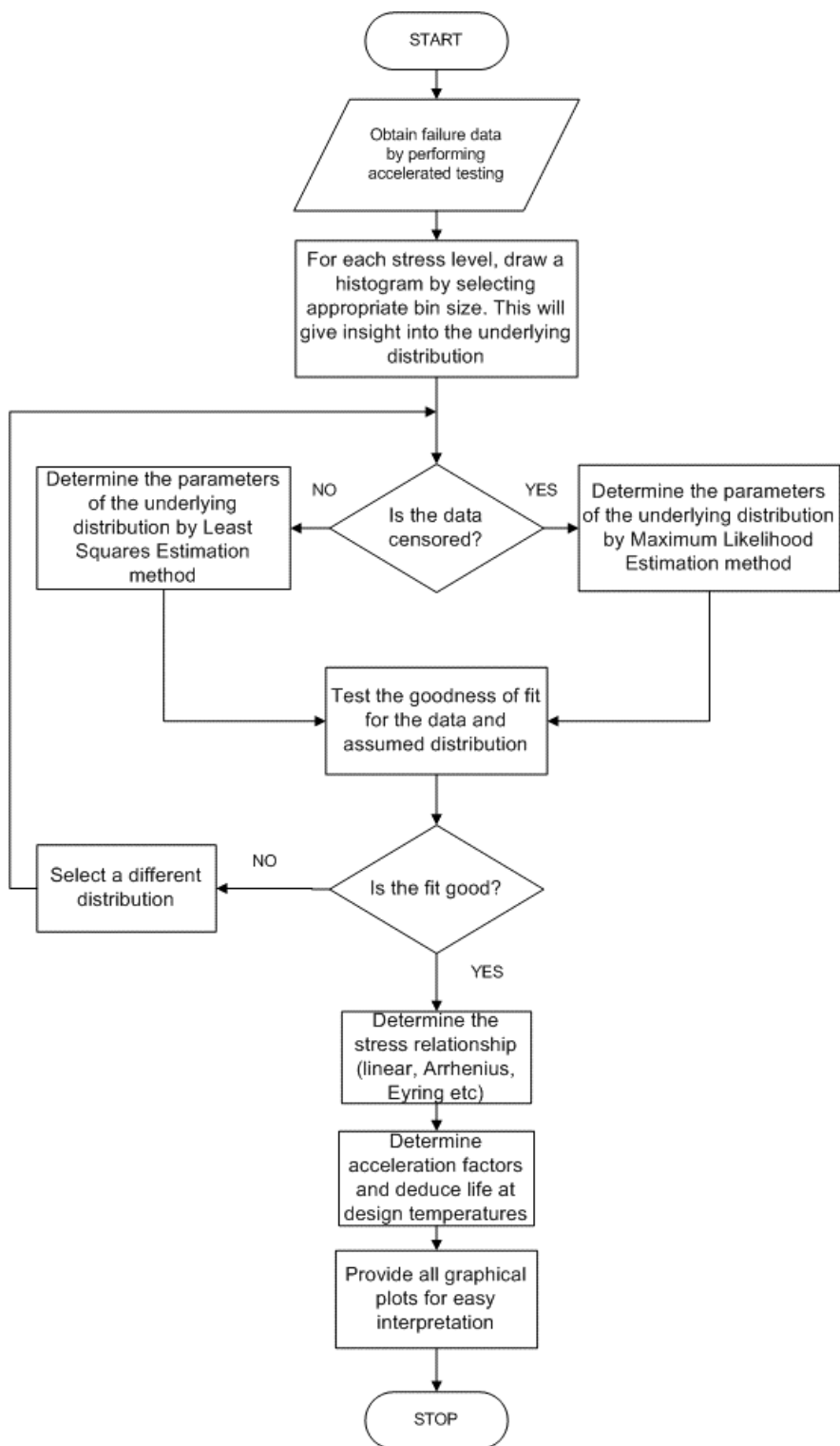


Figure 6.1 Flowchart of statistical analysis for accelerated life tests

As indicated by the flowchart, the first step in analyzing failure data is to draw histograms, which would provide insight into the underlying distribution. In drawing a histogram, it is important to select appropriate bin sizes, and selecting either larger or smaller sizes will distort the shape of the distribution. There is no “correct” method in selecting bin sizes, and many mathematicians have proposed different empirical equations for the selection. The software used to plot the graphs in this chapter is Minitab statistical analysis software version 15 [38].

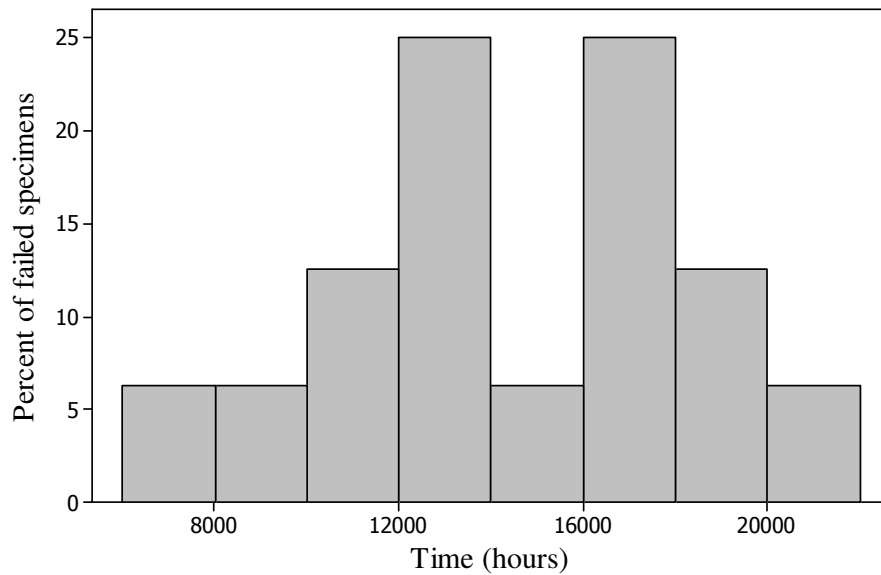


Figure 6.2 Histogram of the failure data at 110 °C



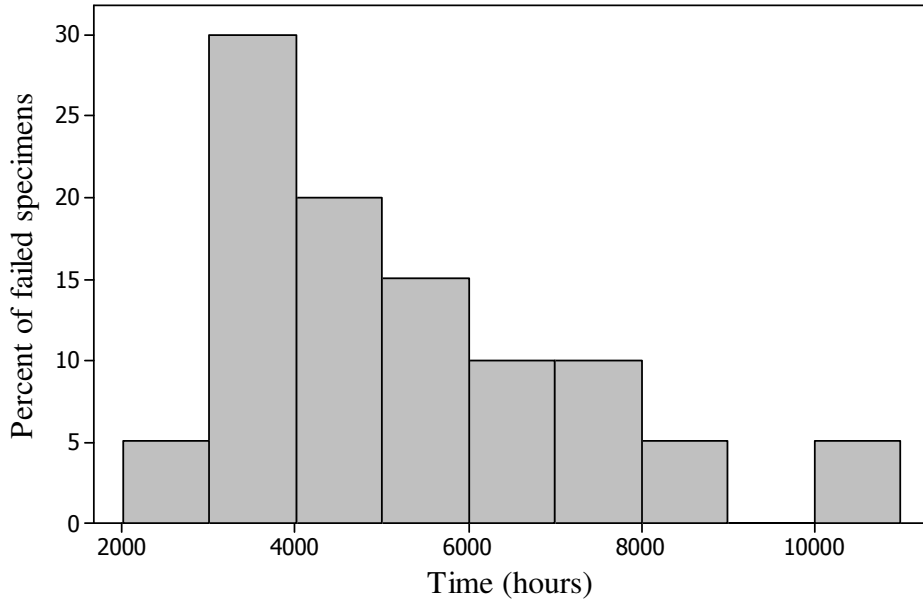


Figure 6.3 Histogram of the failure data at 130 °C

From the histograms above, the data can be suspected to be from normal, lognormal, or Weibull distributions. However, other data distributions, such as exponential, can also be used, and then tested for goodness of fit. Since the data is censored, Maximum Likelihood methods are used to determine the parameters of the distribution. Recall from Chapter 3 that the likelihood estimator is defined as:

$$L(x_1, x_2, x_3, \dots, x_N | A_0, A_1, A_2, \dots, A_k) = \prod_{i=1}^N f(x_i; A_0, A_1, A_2, \dots, A_k) \quad (6.1)$$

For an exponential distribution, estimation of the parameters using MLE is shown as follows. The pdf of an exponential distribution is given by:

$$f(t) = \lambda e^{-\lambda t} \quad (6.2)$$

Applying Equation 6.1, we get:

$$\begin{aligned}
L(\lambda | t_1, t_2, \dots, t_k) &= \prod_{i=1}^N \lambda e^{-\lambda t_i} \\
&= \lambda^N \times e^{-\lambda \sum_{i=1}^N t_i}
\end{aligned} \tag{6.3}$$

Taking the natural logarithm to get the log likelihood estimator, we get:

$$\Lambda = \ln L = N \ln(\lambda) - \lambda \sum_{i=1}^N t_i \tag{6.4}$$

For the log likelihood estimator to be maximum, we find the partial derivative with respect to  $\lambda$  and equate to zero. This will give us an estimate of  $\lambda$  as:

$$\hat{\lambda} = \frac{N}{\sum_{i=1}^N t_i} \tag{6.5}$$

Similarly the estimates of other probability distributions can be determined and is generally done using software as in this problem.

The probability plots for the distributions are shown in Figures 6.3 and 6.4 for 110 °C and 130 °C respectively. The goodness of fit can be determined either graphically or by using the Anderson-Darling (AD). Recall from Chapter 3, that the AD statistic is determined by the equation:

$$A^2 = -N - S \tag{6.6}$$

where  $S = \sum_{k=1}^N \frac{2k-1}{N} [\ln F(T_k) + \ln(1 - F(T_{N+1-k}))]$

This is a very tedious calculation, and generally software is used to calculate the statistic. The test statistics for the distributions in this problem are tabulated in Table 6.2

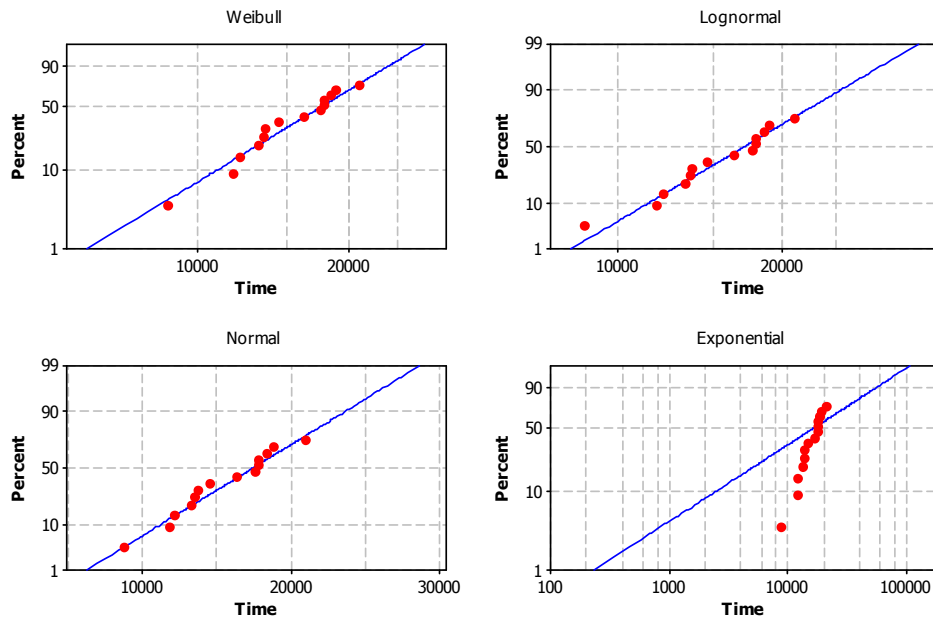


Figure 6.4 Probability plots of the failure data at 110 °C

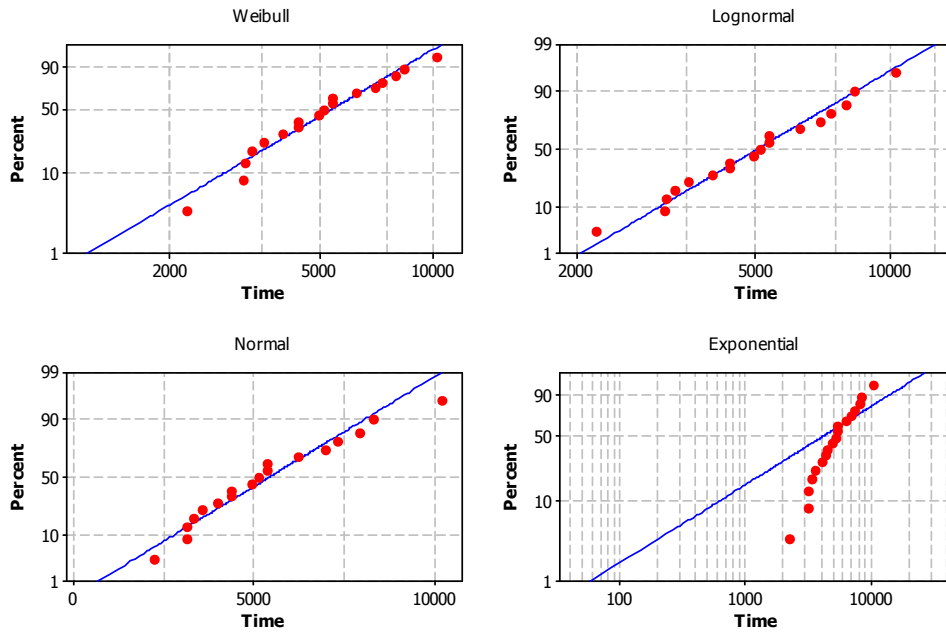


Figure 6.5 Probability plots of the failure data at 130 °C

Table 6.2 Anderson Darling test statistic values

Distribution	AD statistic	
	110 °C	130 °C
Weibull	23.12	1.12
Lognormal	23.10	1.02
Normal	23.11	1.23
Exponential	24.79	3.64

In order to determine goodness of fit graphically, the residuals in the plots in Figures 6.4 and 6.5 need to be carefully observed where the straight line describes the cumulative distribution function form fitting the dataset, on a linearized scale, and the dots are residuals (deviations) of each data point. If all the residual points lie on or around the straight line, then it is a good fit, where as if they are far apart (for example exponential), then the data does not come from that type of distribution. Alternately, by using the Anderson-Darling (AD) test statistic, the goodness of fit can be determined. The AD test statistic is calculated from Equation 3.13 in Chapter 3, and its value should be within specified range of values found in literature for each type of distribution. When the range of values is not available, the distribution with the lowest value of AD statistic fits the data the best. From Table 6.2, it is observed that lognormal distribution describes the data in the problem more closely than any other distribution because the AD value is the least. The mean and standard deviation are determined at each stress level by using maximum likelihood estimation.

The estimates of the lognormal distribution at both temperatures are calculated using software and shown in Figures 6.6 and 6.7

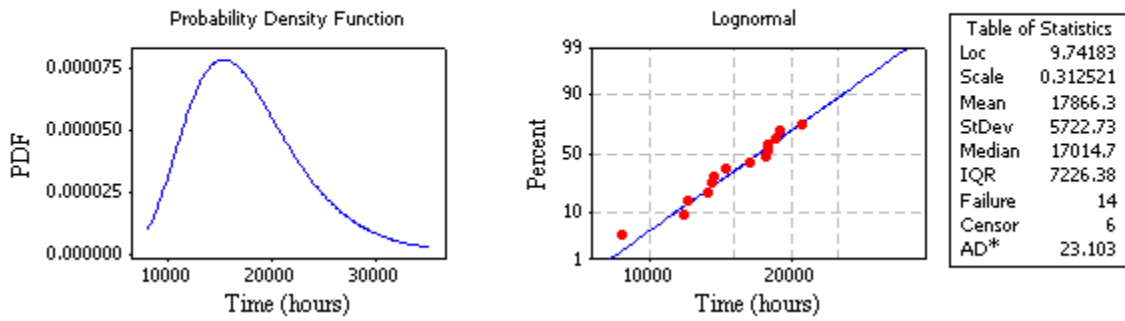


Figure 6.6 Lognormal characteristics of the failure data at 110 °C

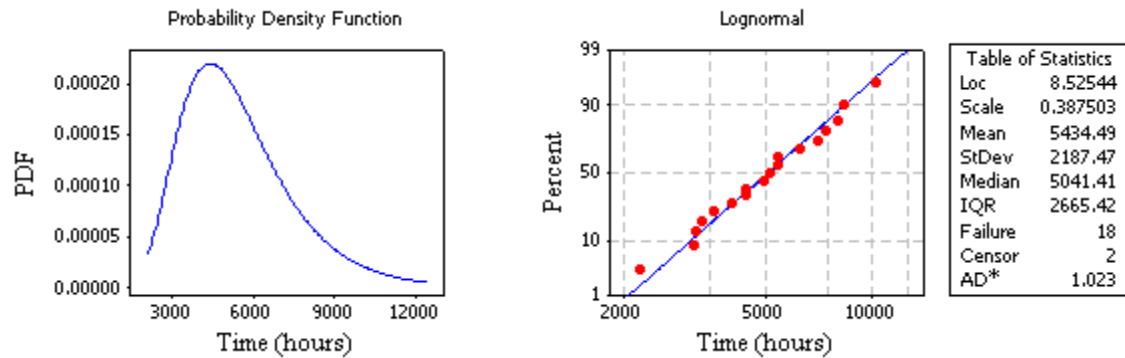


Figure 6.7 Lognormal characteristics of the failure data at 130 °C

From the statistics displayed in Figures 6.6 and 6.7, it observed that the mean life of insulation is 17886 hours at 110 °C and 5434.49 hours at 130 °C. Since the stress is temperature, Arrhenius model can be used to extrapolate life to design conditions. Activation energy for the Arrhenius equation can be calculated from the Equation 6.7

$$E_A = k \cdot \ln \left( \frac{L_1}{L_2} \right) \left( \frac{T_1 T_2}{T_1 - T_2} \right) \quad (6.7)$$

where  $L_1$  and  $T_1$  correspond to life and temperature at one elevated stress

$L_2$  and  $T_2$  correspond to life and temperature at a different elevated stress

$k$  is the Boltzmann's constant ( $8.623 \times 10^5$ )

Substituting the results obtained earlier, we get  $E_A = 0.00669$  eV. Using this value, life at any other stress can be determined using Equation 5.2

$$L_O = L_S e^{\frac{E_A}{k} \left( \frac{1}{T_O} - \frac{1}{T_S} \right)} \quad (6.8)$$

where  $L_O$  and  $T_O$  correspond to life and temperature at the design stress level

$L_S$  and  $T_S$  correspond to life and temperature at the elevated stress level

$k$  is the Boltzmann's constant ( $8.623 \times 10^5$ )

The results for such a calculation have been performed using software and the plot is shown in Figure 6.8

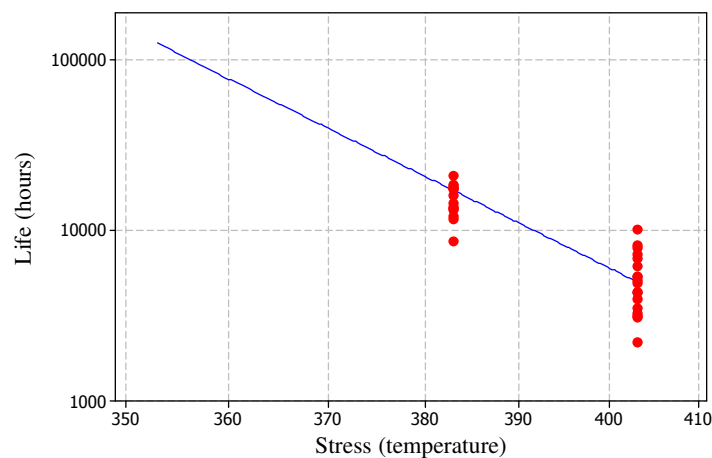


Figure 6.8 Arrhenius plot for cable insulation

From the plot in Figure 6.8, the predicted design life for cable insulation at design temperature of 80°C is 121,368 hours or approximately 13.8 years.

#### Degradation data analysis

The analysis previously conducted describes the analysis method for failure data. Some products and components show degradation characteristics, and in those situations, time and money can be saved by testing the specimens for degradation parameters rather than failures. Degradation beyond a limit can be considered a failure because the device would be rendered useless after those degradation levels. Some of the examples of degradation are light intensity of LEDs, strength of adhesive bonds, etc. Data for degradation analysis of 24 LEDs is shown in the Table 6.3. The accelerating stress is current and the output light intensity decreases with time. The LED's are inspected after every 50 hours up to 250 hours. If this was a failure data test, the specimens would have taken longer to fail and hence prove expensive. Degradation of light intensity below 50 units is considered a failure.

Table 6.3 Degradation data of LEDs

inspection (hours)	Light intensity	current (mA)	unit id
50	86.6	40	1
100	78.7	40	1
150	76	40	1
200	71.6	40	1
250	68	40	1
50	82.1	40	2
100	71.4	40	2
150	65.4	40	2
200	61.7	40	2
250	58	40	2
50	82.7	40	3
100	70.3	40	3
150	64	40	3
200	61.3	40	3
250	59.3	40	3
50	79.8	40	4
100	68.3	40	4
150	62.3	40	4
200	60	40	4
250	59	40	4
50	75.1	40	5
100	66.7	40	5
150	62.8	40	5
200	59	40	5
250	54	40	5
50	83.7	40	6
100	74	40	6
150	67.4	40	6
200	63	40	6
250	61.3	40	6
50	73	40	7
100	65	40	7
150	60.7	40	7
200	58.3	40	7
250	58	40	7
50	86.2	40	8
100	67.6	40	8
150	62.7	40	8
200	60	40	8
250	59.7	40	8
50	81.2	40	9
100	65	40	9
150	60.6	40	9
200	59.3	40	9
250	57.3	40	9
50	66.8	40	10
100	63.3	40	10
150	59.3	40	10
200	57.3	40	10
250	56.5	40	10
50	66.1	40	11
100	64.2	40	11
150	59.4	40	11
200	58	40	11
250	55.3	40	11
50	76.5	40	12
100	61.7	40	12
150	61.3	40	12
200	59.7	40	12
250	56	40	12

inspection (hours)	Light intensity	current (mA)	unit id
50	95.1	35	13
100	86	35	13
150	77.6	35	13
200	70	35	13
250	66.7	35	13
50	93.3	35	14
100	87.1	35	14
150	79.7	35	14
200	74.3	35	14
250	73	35	14
50	98.3	35	15
100	92.4	35	15
150	89	35	15
200	84.3	35	15
250	83	35	15
50	96.6	35	16
100	88.2	35	16
150	85.1	35	16
200	81.4	35	16
250	78.6	35	16
50	95.8	35	17
100	89	35	17
150	84	35	17
200	81	35	17
250	80	35	17
50	94	35	18
100	82.4	35	18
150	77.4	35	18
200	71.7	35	18
250	70.6	35	18
50	88.2	35	19
100	78.7	35	19
150	75	35	19
200	70	35	19
250	69.3	35	19
50	86.7	35	20
100	78	35	20
150	73.3	35	20
200	68.7	35	20
250	67.3	35	20
50	89	35	21
100	80	35	21
150	76.3	35	21
200	72.3	35	21
250	71.3	35	21
50	96.2	35	22
100	86.5	35	22
150	81.4	35	22
200	74.5	35	22
250	74.2	35	22
50	97.5	35	23
100	84.5	35	23
150	81	35	23
200	75	35	23
250	74.1	35	23
50	92.4	35	24
100	85.4	35	24
150	80	35	24
200	73.3	35	24
250	71.5	35	24



In degradation analysis, basic mathematical models are used to extrapolate the performance measurements over time to the point where the product would have degraded beyond critical value. Once this has been determined, analysis can be done with standard life data analysis techniques. For the data above, a linear model is used and the following graph in Figure 6.9 is obtained

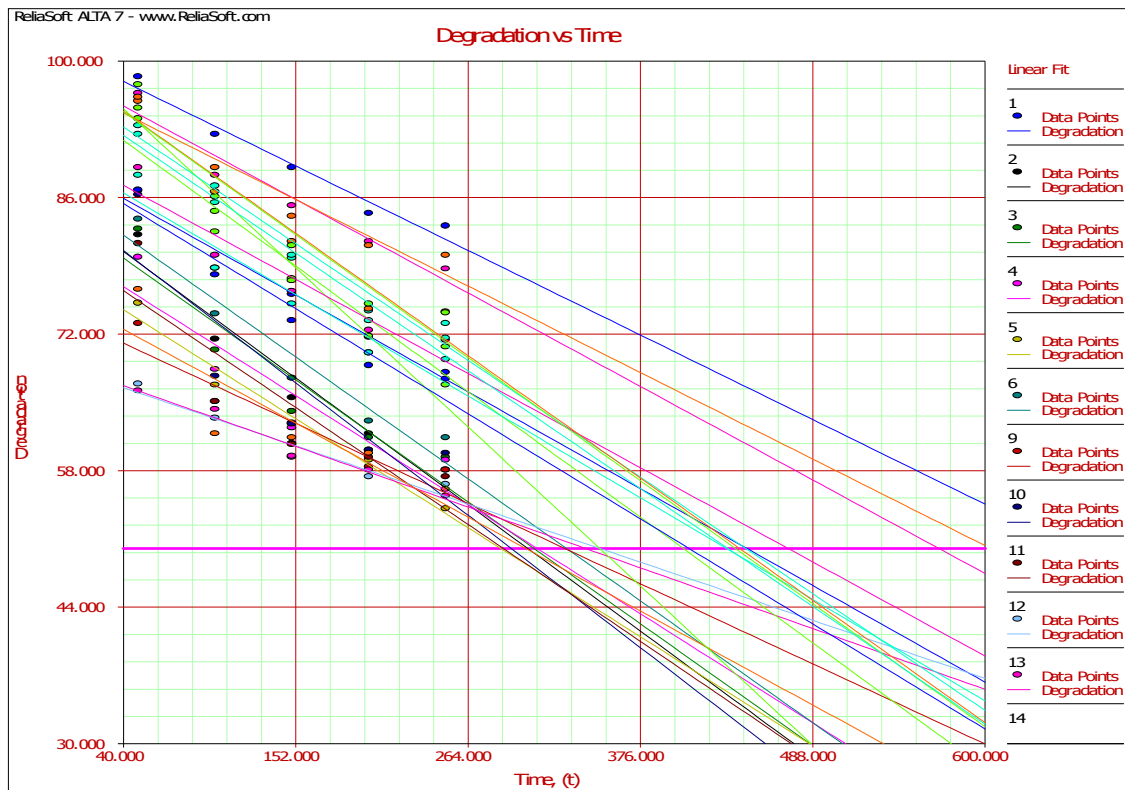


Figure 6.9 Degradation data

From Figure 6.9, most of the LEDs fail as they cross the thick horizontal pink line at 50 units. The points at which they do so are considered their failure times and standard failure data analysis is then performed as performed in the previous example. Recall from Chapter 3 that the inverse power law can be used to determine the relation since the accelerating stress is not temperature. Since the stress in this case is current, the inverse

power law can be used to map the life at operating with 40 mA to a design level of 25 mA. The On solving the problem using the approach shown in the previous example, Figure 6.10 is obtained. It shows the life vs. stress. From the plot, the predicted life at design current of 25 amperes is 1346 hours.

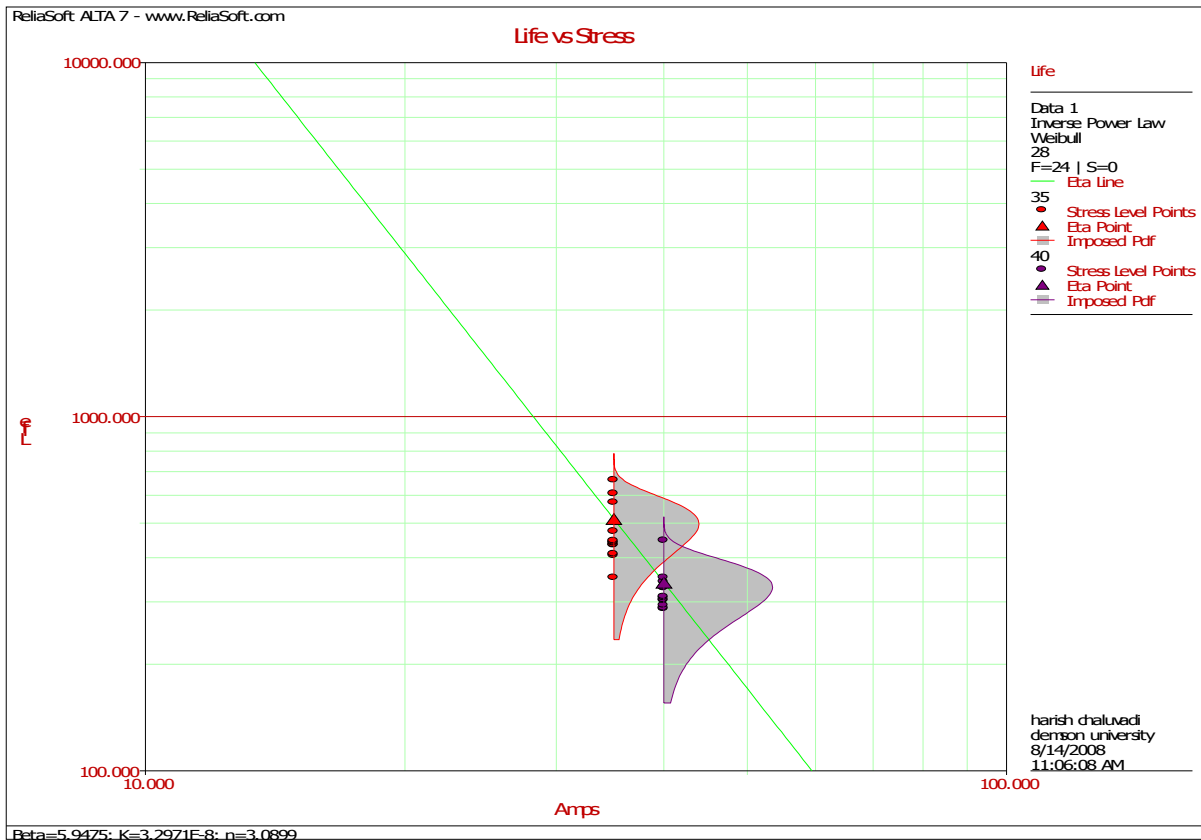


Figure 6.10 Inverse power law plot showing stress vs. life

## CHAPTER 7

### CONCLUSION

Traditionally, electricity consumption was measured using electromechanical watt-hour meters. Many meters, across America, have reached the wear-out stage of their lifespan and require replacements. In the next few years, utilities all over the country intend to replace these old and aging electromechanical meters with state-of-the-art electronic ones on a large scale [35]. Doing so could improve metering accuracy, add security, allow communications (AMI), and facilitate demand response operations in distribution systems. However, the reliability of electronic components has been a concern and many experts believe that the electronic meters will not survive as long as their electromechanical predecessors [35].

This thesis provides a methodology for the prediction of life of electronic meters using accelerated life tests. At first, fundamentals of meter operation are discussed, since knowledge of the construction and operation of the electronic meters is essential to pursue the project further. Operational features and gear ratio constants of traditional electromechanical meters are also discussed because terminology related to calibration is inherited from these electromechanical meters to the new electronic ones.

This is followed by a literature review of accelerated test methods and models. Different data types and corresponding analysis methods are discussed. Failure time distributions along with goodness-of-fit tests are also reviewed. Finally the various life-

stress relationships that are used to map estimates at high stress conditions to the usage conditions, for different types of stresses, are discussed.

Meter failures in the field that would generally occur over many years can be observed at a faster rate by operating them in environmental chambers at elevated stress conditions by a technique known as accelerated life testing (ALT). The methods of analyzing the resulting failure data were also discussed.

The manual inspection of meters on a monthly basis would provide only censored data and would be inadequate for life analysis prediction. A Data Acquisition system (DAQ) was developed to extract data from the interiors of the inaccessible environmental chambers. The DAQ was required to extract information regarding the health of the meters and the temperature from the interior of the environmental chamber. At first, the required design specifications for proper functionality of the DAQ are identified. Based on these specifications, sensors, both infrared phototransistors and thermocouples, are selected. This is followed by an explanation of the details of the instrumentation devices developed for data acquisition. Finally, a Human Machine Interface (HMI), that is used to interface the data acquisition system with software, is built using LabVIEW. The benefits of the layout of the HMI and its functionality have also been illustrated in detail.

In constructing the HMI, a few meters were required to be in an operational state to gain insight into the pulse characteristics i.e., wavelength, width, and rate of occurrence of the pulses. Methods of making the DAQ flexible for operation with any brand of meters were also to be determined. In order to accomplish these tasks, a prototype had to be constructed in Clemson University's PQIA lab that would mimic the

actual test setup at the EPRI facility. The details of the prototype have been discussed in detail.

Then a description of the features and limitations of the test set-up used at the EPRI facility to conduct ALTs were provided. The environmental chamber that is being used at EPRI facility was found to be limited in its operation. In the future, the system needs to be expanded by increasing the environmental chamber's heating and refrigeration capability in order to obtain failure data in a timely fashion.

After six months of testing at a constant stress of 80 °C, no failures were observed in the 20 meters that were being tested. Degradation data revealed the meters to be within the IEC and ANSI design specifications. The EPRI test plan was inadequate for inducing thermal-related failures in the electronic meters, and thus life prediction analysis could not be carried out. The reasons for this have been discussed and remedies are listed in Chapter 5.

Since no failure data was observed during the time devoted to this project, the analysis method determined to predict the life of the electronic watt-hour meters have been illustrated using data from the literature. Two methods of analysis, i.e., traditional failure data analysis and degradation analysis have been illustrated using failure data from cable insulation specimens and LED specimens respectively. When the failure data for the electronic meters is available from future experiments, it can be used, with minimal alterations to the model, to obtain the estimate of life as illustrated using the examples.

### Future work

The data acquisition system described in this thesis was designed with the capability of being expanded, as more phototransistors and thermocouples can be attached when required. Life-stress relationships for stresses other than temperature have also been described in the Chapter 3 and could yield valuable life related information. Lab testing at 80 °C and -35 °C did not reveal any failures. The reason for lack of failures was determined to be the levels of stresses. Both 80 °C and -35 °C fall within the IEC design specifications of electronic revenue meters [22], and in order to observe failures, either the stress level or test duration will need to be increased. Improvements in the test plans by increasing the stress levels can yield better results and these recommendations were made to EPRI.

In the future, a temperature cycling test is to commence with temperature cycled between the two extremes – 80 °C and -35 °C. The test will be conducted for a period of four months and the results, for analysis, will be available by the end of December 2008. The Coffin-Manson life-stress relationship can be used to map the results, if any, to usage level conditions. However, it is unlikely that failures will result from this test because the rate of increase of temperature in the chamber is not high enough to induce thermal shock. The reason for the slow rate of increase was concluded to be because of the large size of the chamber.

Once the dependence of life on temperature is determined, life–stress relationships with other stresses that act on electronic meters in the field should be investigated. In a future phase of this sponsored project, an additional stress, such as

voltage will be added. This will give the correlation between life and both the stresses acting simultaneously on the meter and thus mimic the actual conditions under which the meter operates in the field more closely. The data acquisition system has been made flexible to accommodate any brand of meters and different types of stresses, and thus can be used for all future testing.

## APPENDICES



## Appendix A

### NI SCB 68 breakout board pinout diagram

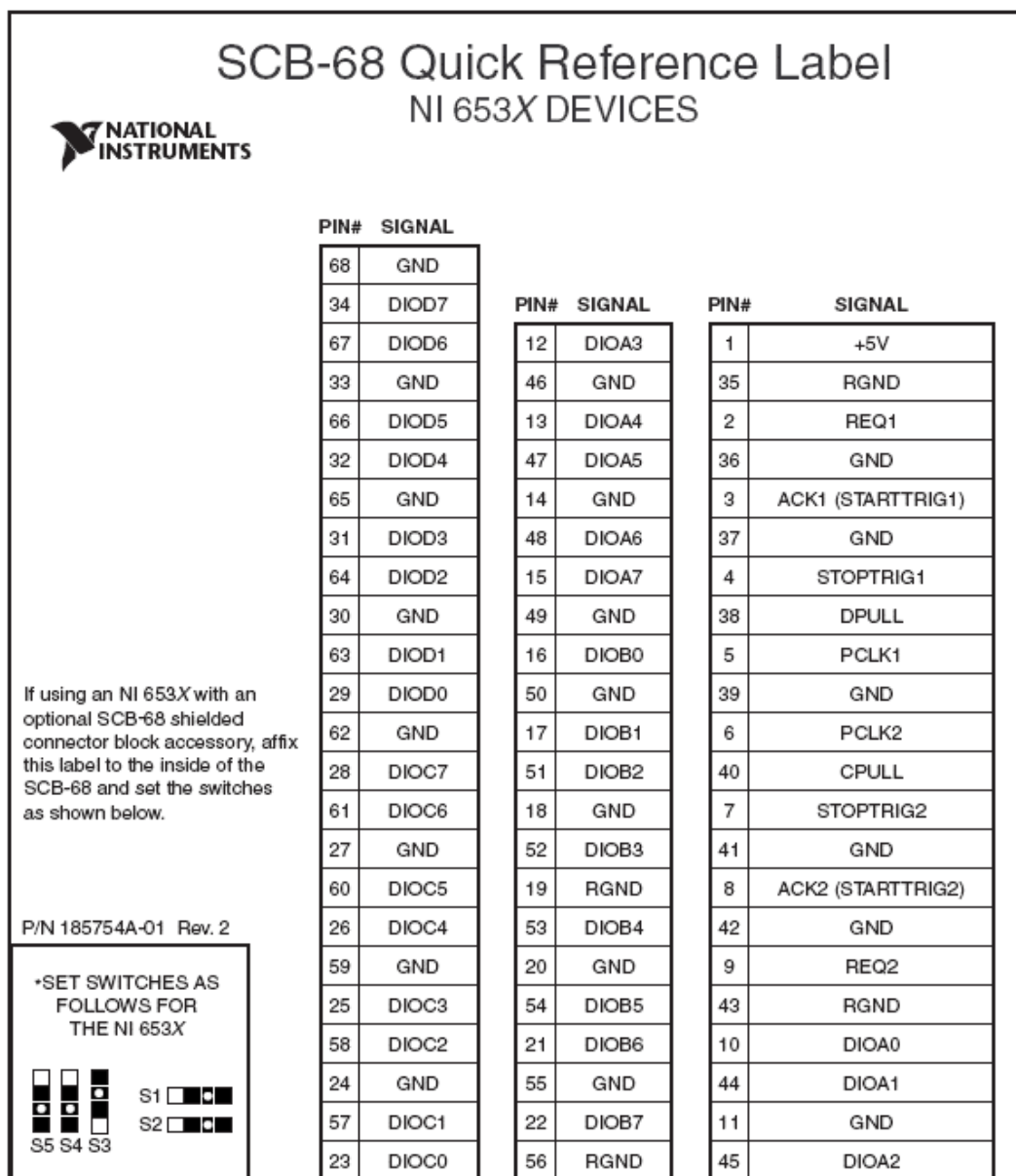


Figure A.1 Pin-out diagram of SCB 68 for NI 653X series  
(Source: NI SCB 68 user manual)

Appendix B

Type T thermocouple coefficients

Temperature range : -200 to 0 °C Voltage range : -5.6 to 0 mV		Temperature range : 0 to 400 °C Voltage range : 0 to 20.87 mV	
coefficients		coefficients	
a <sub>0</sub>	0	a <sub>0</sub>	0
a <sub>1</sub>	25.949192	a <sub>1</sub>	25.928
a <sub>2</sub>	-0.21316967	a <sub>2</sub>	-0.7602961
a <sub>3</sub>	0.79018692	a <sub>3</sub>	0.04637791
a <sub>4</sub>	0.42527777	a <sub>4</sub>	-0.002165394
a <sub>5</sub>	0.13304473	a <sub>5</sub>	6.04814E-05
a <sub>6</sub>	0.020241446	a <sub>6</sub>	-7.29342E-07
a <sub>7</sub>	0.001266817	a <sub>7</sub>	0

Table B.1 Coefficients for voltage to temperature conversion of  
T type thermocouple (Source: www.nist.gov)

$$T = a_0 + a_1 E + a_2 E^2 + a_3 E^3 + a_4 E^4 + \dots + a_n E^n$$

Where  $a_0, a_1, a_2 \dots a_n$  are coefficients from the Table B.1

$E$  is the emf or voltage observed in mV

$T$  is the temperature in °C

# Appendix C

## LabVIEW program

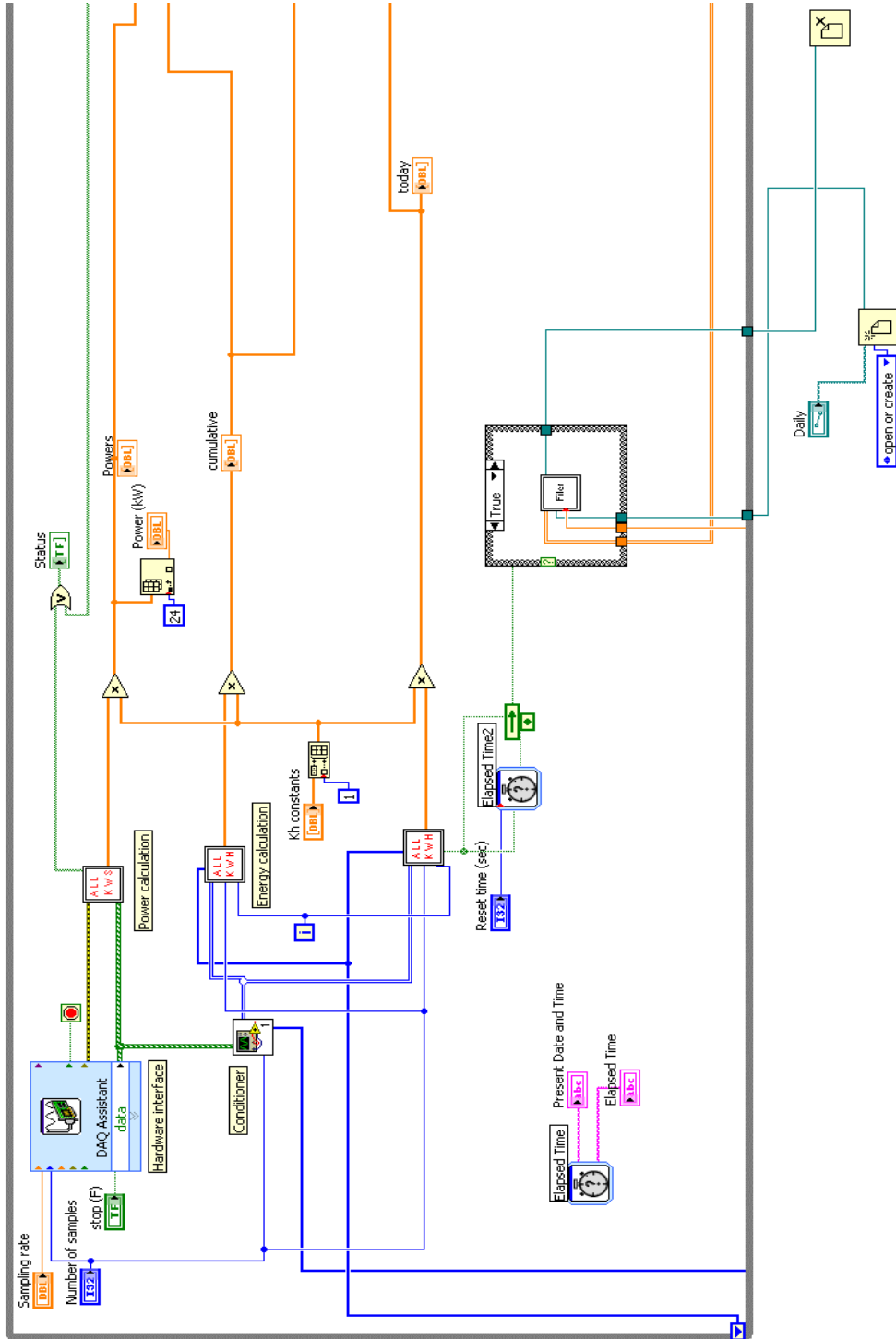


Figure C.1 LabVIEW code for DAQ software

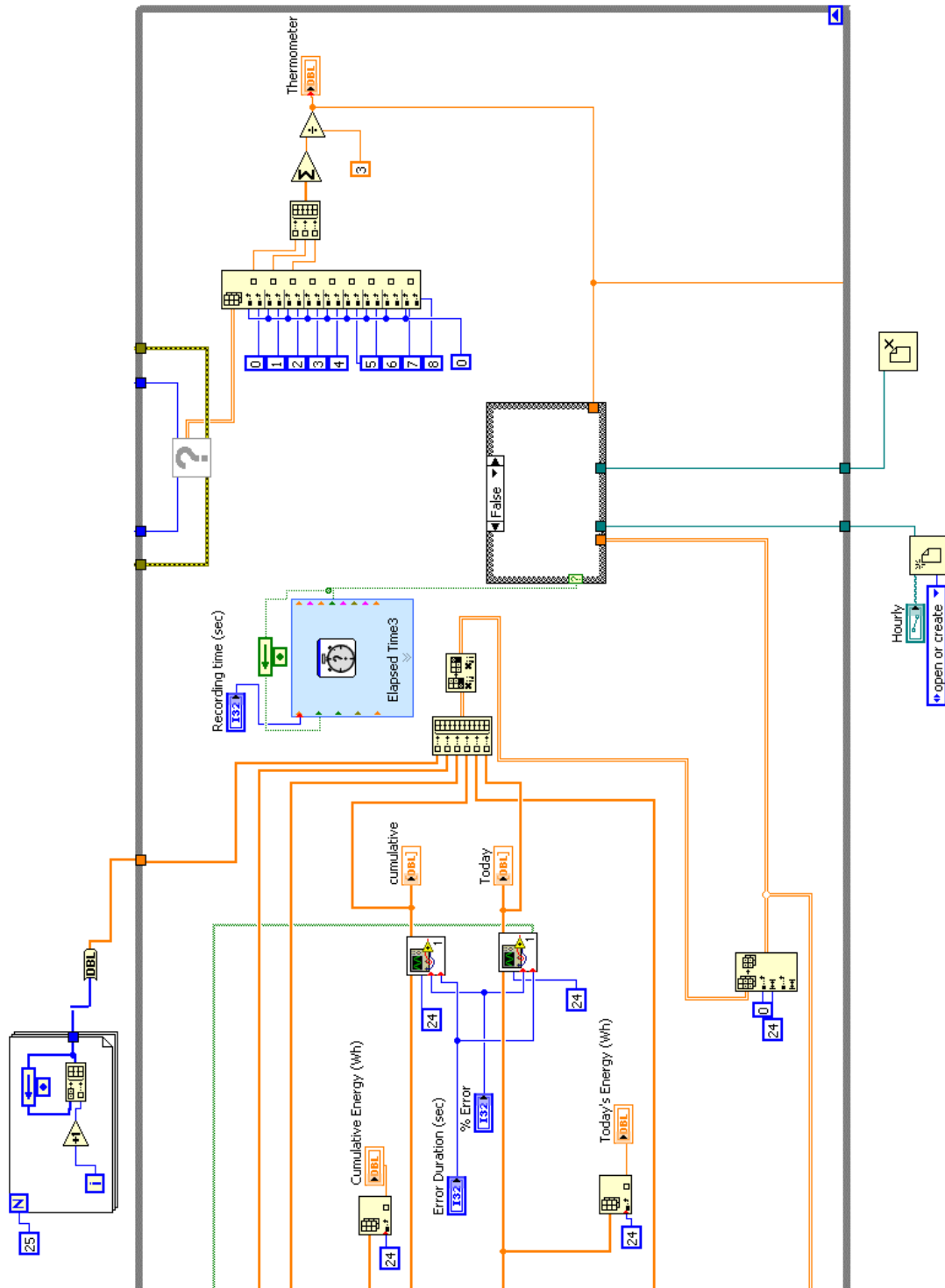


Figure C.2 LabVIEW code for DAQ software (continued)

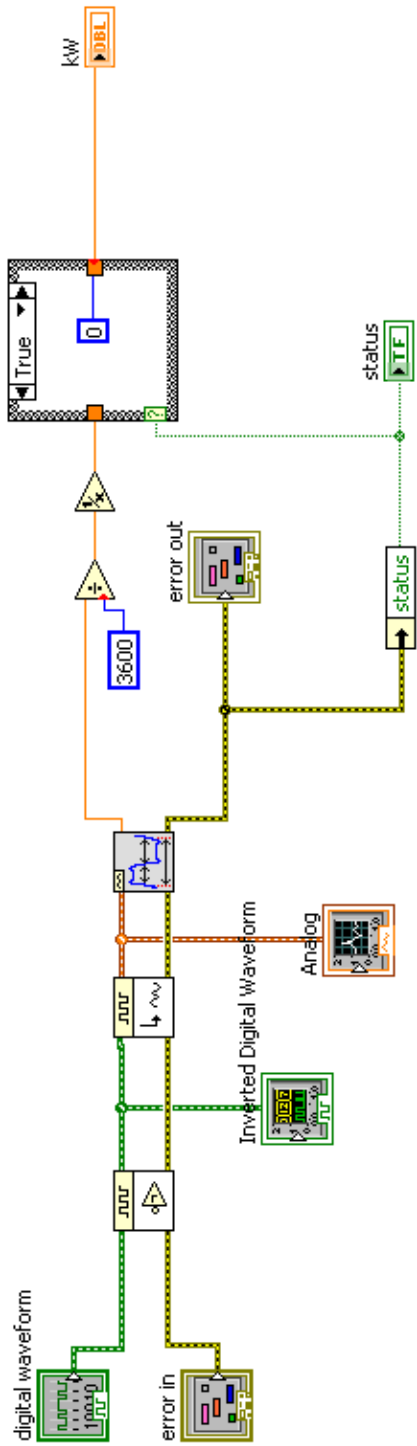


Figure C.3 Function for calculating power

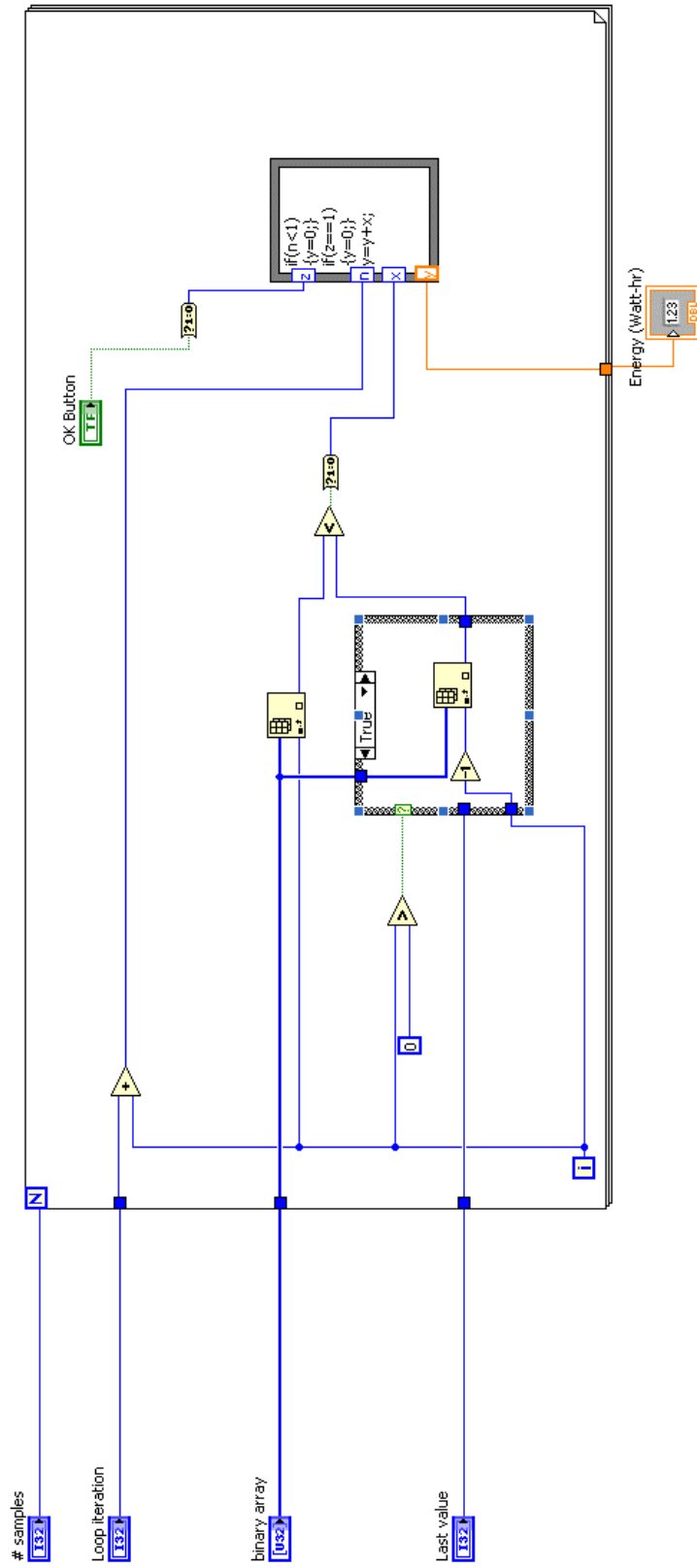


Figure C.4 LabVIEW function for calculating energy (pulse count)

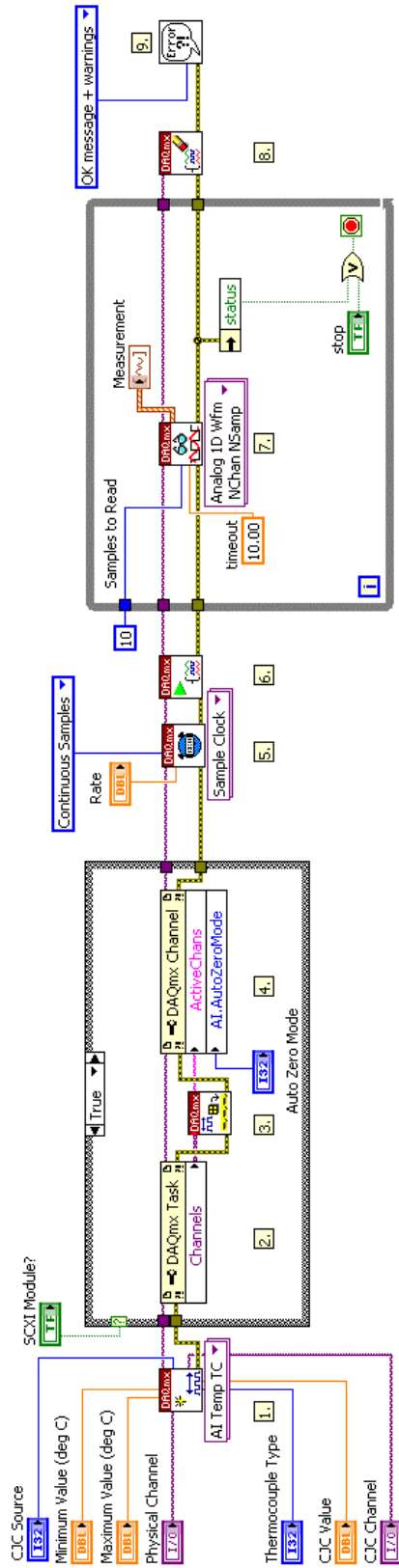


Figure C. 5 LabVIEW function for temperature calculation

## REFERENCES

- [1] *A brief history of meter companies and meter evolution*, Website : <http://watthourmeters.com/history.html> (accessed 07/04/2008).
- [2] United States Energy Policy Act 2005, Website: <http://www.epa.gov> (accessed 07/08/08).
- [3] W. B. Nelson, *Accelerated Testing: Statistical models, Test Plans and Data Analysis*, 2nd ed., New York NY: John Wiley and Sons, 1990.
- [4] E. A. Elsayed, *Reliability Engineering*, Pearson Education, 1996.
- [5] W.Q Meeker and L.A Escobar, *Statistical Methods for Reliability Data*, New York NY: John Wiley and Sons, 1998.
- [6] United States Bureau of reclamation, *Watt-hour meter maintenance and testing*, FIST 3-10, 1992.
- [7] N.Wan and K. Manning, “Exceeding 60-Year Life Expectancy from an Electronic Energy Meter”, *Metering Asia Pacific Conference*, Feb 2001.
- [8] American National Standards Institute, *Code for electricity metering, C12.1*, 2001.
- [9] E. Suhir, “Accelerated Life Testing in Photonics Packaging: Objectives, Role, Attributes, Challenges, Pitfalls, Predictive Models, and Interaction with Other Accelerated Stress Categories”, *SPIE*, 2002.
- [10] NIST/SEMATECH *e-Handbook of Statistical Methods*, Website: <http://www.itl.nist.gov/div898/handbook/> (accessed 07/08/08).
- [11] H. Cui, “Accelerated Temperature Cycle Test and Coffin-Manson Model for Electronic Packaging”, *IEEE RAMS*, 2005.
- [12] L. A. Escobar and W. Q. Meeker, “Statistical Prediction Based on Censored Life Data”, *Technometrics*, vol. 41, no. 2, pp. 113-124, May 1999.
- [13] W. B. Nelson, “Analysis of Accelerated Life Test Data – Part I: The Arrhenius Model and Graphical Methods”, *IEEE Transactions on Electrical Insulation*, vol. EI-6, no. 4, pp. 165-181, Dec. 1971.



- [14] W. B. Nelson, “Analysis of Accelerated Life Test Data – Part II: Numerical Methods and Test Planning”, *IEEE Transactions on Electrical Insulation*, vol. EI-7, no. 1, pp. 36-55, Dec. 1972.
- [15] W. B. Nelson, “Analysis of Accelerated Life Test Data – Part III: Product Comparisons and Checks on the Validity of the Model and the Data”, *IEEE Transactions on Electrical Insulation*, vol. EI-7, no. 2, pp. 99-119, Jun. 1972.
- [16] W. Q. Meeker and G. J. Hahn , “A Comparison of Accelerated Test Plans to Estimate the Survival Probability at a Design Stress”, *Technometrics*, vol. 20, no. 3, pp. 245-247, Aug. 1978.
- [17] W.Q Meeker and L.A Escobar, “Using Accelerated Tests to Predict Service Life in Highly-Variable Environments”, *Invited 71: Quality and reliability improvement*, vol. 21, no. 4, pp. 245-247, Aug. 1980.
- [18] W.Q Meeker and L.A Escobar, “Statistical Methods for Reliability Data Using SAS Software”, *Technometrics*, vol. 20, no. 3, pp. 245-247, Aug. 1978.
- [19] J. W. Park, “Case Studies on the Accelerated Life Tests for the Semiconductor Devices Tests Devices”, *The 16th ISRC Workshop*
- [20] W. M. Shepard and A. G. Jones, *The Watthour Meter*, Technical publishing company, 1910.
- [21] *Handbook for Electricity Metering*, Edison Electric Institute, 9<sup>th</sup> edition, Aug. 1999.
- [22] Electricity metering equipment (AC) – General requirements, tests and test conditions –Part 11: Metering equipment, *International Electrotechnical Commission*, 62052-11, 2003.
- [23] Electricity metering equipment (AC) – Particular requirements – Part 21: Static meters for active energy (classes 1 and 2), *International Electrotechnical Commission*, 62053-21, 2003.
- [24] Electricity metering equipment (AC) – Particular requirements – Part 11: Electromechanical meters for active energy (classes 0.5, 1 and 2), *International Electrotechnical Commission*, 62053-11, 2003.
- [25] Electricity metering equipment (AC) – Particular requirements – Part 31: Pulse output devices for electromechanical and electronic meters (two wires only), *International Electrotechnical Commission*, 62053-31, 1998.

- [26] J. Sethuraman and N. D. Singpurwalla, "Testing for Hypotheses for Distributions in Accelerated Life Tests", *Journal of the American Statistical Association*, vol. 77, no. 377, Theory and Methods Section, Mar. 1982.
- [27] *Analog Devices Reliability Handbook*. Website: <http://www.analog.com> (accessed 07/05/2008).
- [28] V. Ricci, *Fitting Distributions with R*, Release 0.4, Feb. 2005.
- [29] N. H. Criscimagna, "Accelerated Testing", *Selected Topics in Assurance Related Technologies*, vol. 6, no. 4, Apr. 1999.
- [30] *Life data Analysis reference*, Website: [www.weibull.com](http://www.weibull.com) (accessed 07/04/2008), Updated: Apr. 2007.
- [31] *Accelerated Life Testing reference*, Website: [www.weibull.com](http://www.weibull.com) (accessed 07/04/2008), Updated: Apr. 2007.
- [32] C. R. Yang and J. T. Kim, "Temperature Accelerated Life Test (ALT) at the Circuit Board Level", *IEEE International Electronics Manufacturing Technology Symposium*, Apr. 1995.
- [33] W. J. Minford, "Accelerated Life Testing and Reliability of High K Multilayer Ceramic Capacitors", *IEEE transactions on Components, Hybrids, Manufacturing Technology*, vol. CHMT-5, pp. 297-300, Sep 1982.
- [34] J. P. Rooney, "Aging in Electronic Systems", *Proceedings of the Annual Reliability and Maintainability Symposium*, pp. 293-299, Aug. 1999.
- [35] *Accelerated Life Testing of Solid-State Residential Meters: Technical Update*, EPRI, Palo Alto, CA: 2006. 1012440.
- [36] *Obsolescence Planning of Domestic Electronic Meters*. EPRI, Palo Alto, CA: 2006. 1012441.
- [37] *Accelerated Life Testing of Domestic Solid-State Residential Meters*. EPRI, Palo Alto, CA: 2007. 1013968.